



MARMARA UNIVERSITY
FACULTY OF ENGINEERING



**DESIGN OF A FLEXIBLE 3 DOF FORCEPS
MECHANISM FOR ROBOTIC SURGERY**

HAMZA ÖZDEMİR, BÜNYAMİN NACİ SEFEROĞLU, EMİRHAN
ÇANDAR

GRADUATION PROJECT REPORT
Department of Mechanical Engineering

Supervisor
Assoc. Prof. Uğur TÜMERDEM

ISTANBUL, 2024



**MARMARA UNIVERSITY
FACULTY OF ENGINEERING**



**DESIGN OF A FLEXIBLE 3 DOF FORCEPS MECHANISM
FOR ROBOTIC SURGERY
BY**

**HAMZA ÖZDEMİR, BÜNYAMİN NACİ SEFEROĞLU
EMİRHAN ÇANDAR**

June 2024, Istanbul

**SUBMITTED TO THE DEPARTMENT OF MECHANICAL ENGINEERING IN
PARTIAL FULFILLMENT OF THE REQUIREMENTS FOR THE DEGREE OF
BACHELOR OF SCIENCE AT MARMARA UNIVERSITY**

The author(s) hereby grant(s) to Marmara University permission to reproduce and to distribute publicly paper and electronic copies of this document in whole or in part and declare that the prepared document does not in anyway include copying of previous work on the subject or the use of ideas, concepts, words, or structures regarding the subject without appropriate acknowledgement of the source material.

Signature of Author(s)

Department of Mechanical Engineering

Certified By

Project Supervisor, Department of Mechanical Engineering

Accepted By

Head of the Department of Mechanical Engineering

Acknowledgement

First of all, We would like to thank our supervisor Dr. Uğur TÜMERDEM for the valuable guidance and advice on preparing this thesis and giving me moral and material support.

June , 2024

HAMZA ÖZDEMİR
BÜNYAMİN NACİ SEFEROĞLU
EMİRHAN ÇANDAR

Acknowledgement	i
1. Abstract	5
2. Symbols and Abbreviations	6
3. List of Figures and Tables.....	7
4. History of robotic surgery	9
5. Introduction	10
5.1. What is the Soft Robotic ?.....	11
5.2. What is Forceps?	12
5.3. What is Ansys?.....	12
5.4. What Does Ansys Analysis Do ?	13
5.5. What is SolidWorks?.....	13
5.6. What Does SolidWorks Do ?	14
6. Materials and methods	14
6.1. Stainless Spring Steel (1.8159)	14
6.2. Aluminum.....	16
6.3. Steel	16
6.4. Ni-Ti	16
7. Current status and related studies.....	17
7.1. 3.5 mm compliant robotic surgical forceps with 4 DOF : design and performance evaluation D. S. V. Bandara, Ryu Nakadate, Murilo M. Marinho, Kanako Harada, Mamoru Mitsuishi & Jumpei Arata	17
7.2. Sensored Surgical Forceps for Robotically Assisted Minimally Invasive Surgery Authors: Kim, Uikyum; Kim, Yong Bum; So, Jinho; Seok, Dong-Yeop; Choi, Hyouk Ryeol	
	18

7.3.	Lyapunov-based bilateral teleoperation for surgical robotic forceps system with time varying delay Authors: Ishii, Chiharu; Mikami, Hiroyuki; Nishitani, Yosuke.....	19
7.4.	A New Type of Surgical Forceps Integrated with Three-Axial Force Sensor for Minimally Invasive Robotic Surgery Authors: Kim, Uikyum; Kim, Yong Bum; Seok, Dong-Yeop; So, Jinho; Choi, Hyouk Ryeol.....	20
7.5.	Force Sensor Integrated Surgical Forceps for Minimally Invasive Robotic Surgery Authors : Kim, Uikyum; Lee, Dong-Hyuk; Yoon, Woon Jong; Hannaford, Blake; Choi, Hyouk Ryeol	21
7.6.	Meta-analysis of observational studies on the safety and effectiveness of robotic gynaecological surgery Authors:M. Reza; S. Maeso; J. A. Blasco; E. AndradasM. Reza; S. Maeso; J. A. Blasco; E. Andradas	23
7.7.	Transanal specimen extraction in robotic rectal cancer surgery Authors:J. Kang; B. S. Min; H. Hur; N. K. Kim; K. Y. Lee	23
8.	Design.....	24
9.	Motion	27
10.	Kinematic Model.....	28
10.1.	For Bending (α).....	28
10.2.	For Bending (β)	30
10.3.	For Grasping (γ)	31
10.4.	Overall kinematic model	32
11.	Finite Element Analysis	33
11.1.	Material properties(Stainless Spring Steel (1.8159, 51CrV4))	34
11.2.	For $\alpha =15$ degree	34
11.3.	For $\alpha =30$ degree	36
11.4.	For $\alpha =45$ degree	38
11.5.	For $\alpha =15^\circ ; \gamma=15^\circ$	40
11.7.	Optimization.....	44
11.7.1.	Comparison of nickel titanium and stainless spring steel	45
11.7.2.	Optimization of stainless spring steel according to its thickness	47

12.	Work Space	50
13.	Manufacturability	54
14.	Discussion and Conclusion	58
15.	References	59

1. Abstract

The subject of this project is Compliant Robotic Surgical Forceps With 3 DOF. First, similar drawings of robotic arms were examined. Since the working areas of robotic arms are quite limited, it was investigated where and in what environments they should be used. It was observed whether the drawings were related to the subject or not. First, the drawing of the robotic arms started on the SolidWorks platform. The drawings made on the SolidWorks platform were analyzed on the Ansys platform. The analyzes obtained from the Ansys program were evaluated and tested for suitability to the calculations. Then, the working area of the mechanism began to be calculated. The working area calculation of robotic arms was calculated manually by ourselves using formulas. Since the working area of the robotic arms is quite sensitive and meticulous, careful and zero-error calculations were made.

2. Symbols and Abbreviations

Ni: Nickel

Ti: Titanium

Ti-Ni: Nickel-Titanium

NOL: Naval Ordnance Laboratory

DOF: Degree of freedom

İMES: İstanbul Madeni Eşya Sanatkârları Sanayi Odası

3D: 3 dimensional

3. List of Figures and Tables

Figure 1:History of robotic surgery.....	9
Figure 2:Robotic surgery forceps	11
Figure 3: robotic surgical forceps with 4 DOF	18
Figure 4: Locations of force sensors on a surgical instrument. (a) The forceps composed of two jaws. (b) Teeth region and proximal region on a jaw.....	19
Figure 5: DSD forceps teleoperation system (see online version	20
Figure 6: Actual picture of the forceps composing the two	21
Figure 7: (a) Entire surgical instrument. (b) Three-dimensional model of gripper. (c) Three-dimensional model of articulated joint.....	22
Figure 8: a)M5 screw b)Cylinder(head) c)pin d)Stainless spring steel e)scissors with spring.....	24
Figure 9: Assembly stages	26
Figure 10: movement of design.....	27
Figure 11: Overview of the kinematic structure α bending.....	28
Figure 12: Overview of the kinematic structure β bending.....	30
Figure 13: Overview of the kinematic structure γ , grasping.....	31
Figure 14:a and b) Analysis for 15 degrees c) Von mises values for 15 degrees d) Distance values for 15 degrees e) estrn values for 15 degrees.....	35
Figure 15: a and b) Analysis for 30 degrees c) Von mises values for 30 degrees d) Distance values for 30 degrees e) estrn values for 30 degrees.....	37
Figure 16: a and b) Analysis for 45 degrees c) Von mises values for 45 degrees d) Distance values for 45 degrees e) estrn values for 45 degrees.....	39
Figure 17: a and b) Analysis for 15 degrees c) Von mises values for 15 degrees d) Distance values for 15 degrees e) estrn values for 15 degrees.....	41
Figure 18: a and b) Analysis for 15 degrees c) Von mises values for 15 degrees d) Distance values for 15 degrees e) estrn values for 15 degrees.....	43
Figure 19: Max von mises values of stainless spring steel for 30 degrees	45
Figure 20: Maximum Von mises values of nickel titanium for 30 degrees	45
Figure 21: Max Von mises values of nickel titanium for 45 degrees	46
Figure 22: Max Von mises values of nickel titanium for 57 degrees	46
Figure 23: Analysis of stainless spring steel with 2 mm thickness at 30 degree	47
Figure 25: Analysis of stainless spring steel with 0,50 mm thickness at 30 degree	48

Figure 25: Analysis of stainless spring steel with 0,6 mm thickness at 30 degree	48
Figure 26: Analysis of the maximum angle that can be reached at 0.85 at 30 degrees	49
Figure 27: Scissor movement kinematic analysis	50
Figure 28:work space drawing with AutoCAD	51
Figure 29:analysis of 30 degree displacement	52
Figure 30: first cylinder (head part)	54
Figure 31: 3D printer prototype of scissors.....	55
Figure 32: shaft and stainless steels mounted on the cylinder	56
Figure 34: production of design	57
Figure 34: Assembly of the second cylinder design	57

4. History of robotic surgery

The development of robotic-assisted surgical technology is closely linked to the history of robotic forceps surgery. The introduction and FDA approval of the da Vinci Surgical System in 2000 by Intuitive Surgical marked a turning point in this story. Robotic arms fitted with a range of surgical equipment, such as forceps, were included into the da Vinci System, which transformed surgical processes. During minimally invasive procedures, these forceps, which were operated by a surgeon using a console, offered unmatched precision and dexterity. The da Vinci Surgical System was used in a variety of medical specialties, including general, gynecological, urological, and cardiac surgery. The global deployment of robotic forceps surgery has demonstrated its transformative power, providing advantages including improved visibility, less invasiveness, less blood loss, and quicker recovery periods. Robotic surgical technology is always evolving, which highlights the constant efforts to improve on current systems and discover new areas of minimally invasive surgery. Notwithstanding obstacles like financial concerns and the requirement for thorough training, the development of robotic forceps surgery signifies a paradigm change in favor of increasingly complex and patient-centered surgical techniques.

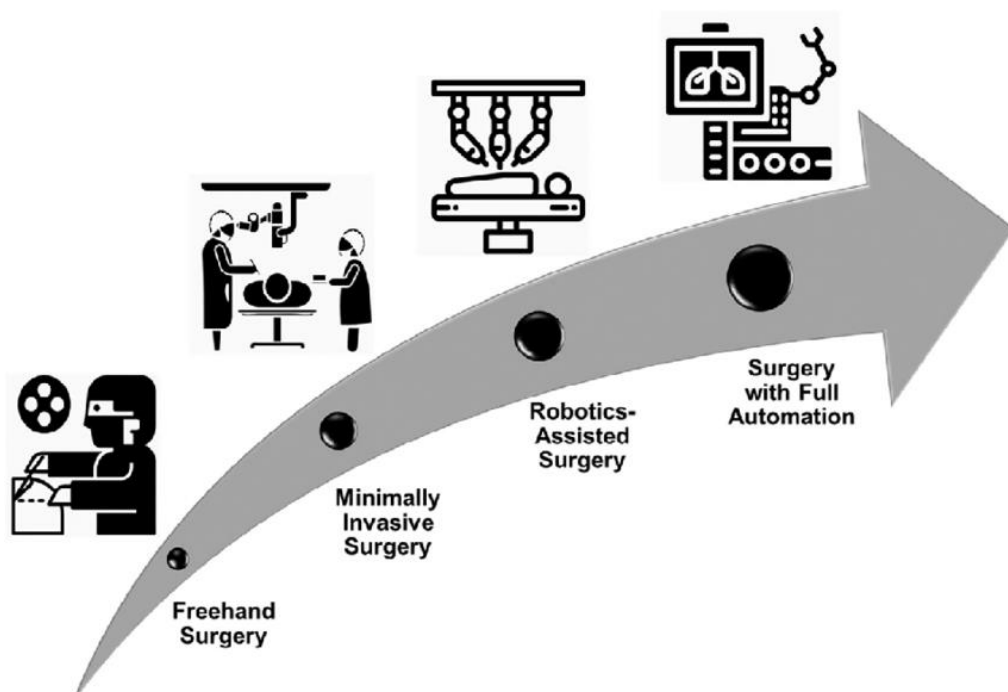


Figure 1:History of robotic surgery

5. Introduction

Robotic surgery, often known as robot-assisted surgery, is a cutting-edge medical technique in which robotic devices are used to aid in surgical procedures. By providing surgeons with greater control, flexibility, and precision during procedures, these technologies are intended to enhance their abilities. Reducing invasiveness, speeding recuperation, and enhancing the efficiency of general surgery are the three main goals of robotic surgery.

People go to hospitals and doctors when they are ill or have a congenital issue in order to get well. They want the surgeries to go smoothly since it won't jeopardize their health, but because surgeons are only human and can't maneuver well in confined spaces, they can't always reach specific places during certain procedures, which increases the likelihood that they will make mistakes. In this project, a robotic arm design that can operate on three axes and much smaller points was created so that the same surgeon could more smoothly and successfully do a difficult procedure that they are unable to perform again. The surgeon's job will be significantly more successful thanks to the robotic arm's multi-axis movement. As a result, there will be a greater chance that the surgeon will perform the procedure successfully and fewer patients will sustain injuries during surgery.

Robotic surgery, which combines the expertise of highly skilled surgeons with the precision of robots, is the pinnacle of medical technology advancement. This new method, also known as robot-assisted surgery, uses robotic technology to perform a variety of surgical procedures. Surgeons operate these devices with robotic arms fitted with specialized equipment from the console. High-resolution 3D cameras are included because they give the surgeon an extended and distinct view of the operating site, which makes it easier for them to operate around intricate anatomical structures. One of the key benefits of minimally invasive surgery is the significance surgeons place on being able to execute intricate procedures with tiny incisions.

While doing this study, we used many computer programs such as Ansys and solidworks. We analyzed the part we drew in Ansys SolidWorks and made our design according to the analysis results and added it to our report.



Figure 2:Robotic surgery forceps

5.1. What is the Soft Robotic ?

The term "soft robotics" describes robotic systems with flexible and adaptable movement capabilities that are constructed from soft materials. Soft robots operate using flexible materials and fluids or gasses, in contrast to conventional rigid robots.

They can move in a more organic and biomimetic manner thanks to these characteristics. In general, soft robotic systems have the following qualities:
Flexibility and Adaptability: Soft robots are more able to adjust to their environment and the forces acting upon them when they are made of soft materials.
Safety: Soft materials lower the chance of harm in robotic systems that interact with people.

Biomimetic Design: Soft robots can imitate the movements and functions of living organisms by drawing inspiration from nature. For example, they can move in multiple directions like an octopus's arms.

New Movement Capabilities: They can perform complex and adaptive movements that traditional robots cannot achieve.

Medical devices, prostheses, industrial automation, search and rescue missions, and many more fields are among the application areas for soft robots. Their ability to move precisely and adaptably makes them perfect for a wide range of creative solutions.

5.2. What is Forceps?

Robotic surgery, which combines the expertise of highly skilled surgeons with the precision of robots, is the pinnacle of medical technology advancement. This new method, also known as robot-assisted surgery, uses robotic technology to perform a variety of surgical procedures. Surgeons operate these devices with robotic arms fitted with specialized equipment from the console. High-resolution 3D cameras are included because they give the surgeon an extended and distinct view of the operating site, which makes it easier for them to operate around intricate anatomical structures. One of the key benefits of minimally invasive surgery is the significance surgeons place on being able to execute intricate procedures with tiny incisions.

5.3. What is Ansys?

Ansys is a leading engineering simulation software suite that helps engineers design, analyze, and optimize products across a wide range of industries. It's essentially a powerful tool that allows engineers to virtually test and predict how their designs will perform in real-world conditions before they're even built.

Here are some of the benefits of using Ansys:

Reduced development time and costs: By identifying potential problems early in the design process, Ansys can help to avoid costly physical prototypes and late-stage design changes.

Improved product performance: Ansys can help engineers to design products that are stronger, lighter, more efficient, and more reliable.

Enhanced innovation: Ansys can help engineers to explore new design possibilities that would be too difficult or expensive to test physically. Ansys is used by a wide range of companies in a variety of industries, including:

Aerospace: Ansys is used to design and analyze aircraft structures, engines, and landing gear.

Automotive: Ansys is used to design and analyze car bodies, engines, and safety systems.

Biomedical: Ansys is used to design and analyze medical devices, implants, and prosthetics.

Electronics: Ansys is used to design and analyze electronic components and circuits.

Energy: Ansys is used to design and analyze power plants, wind turbines, and other energy infrastructure.

Overall, Ansys is a powerful tool that can help engineers to design better products faster and more efficiently. If you're interested in learning more about Ansys, I recommend visiting the company's website or watching some of their tutorials on YouTube.

5.4. What Does Ansys Analysis Do ?

Here's a breakdown of what Ansys does:

Finite element analysis (FEA): This is the core technology behind Ansys. FEA involves dividing a complex object into smaller, simpler elements (think of them like tiny building blocks) and then analyzing how those elements interact with each other under various loads and conditions. By understanding these interactions, engineers can predict how the entire object will behave.

Multiphysics simulation: Ansys can go beyond just analyzing simple mechanics. It can also simulate complex interactions between different physical phenomena, such as heat transfer, fluid flow, electromagnetism, and more. This allows engineers to design products that are not only structurally sound but also perform optimally in their intended environment.

5.5. What is SolidWorks?

SolidWorks is one of the leading 3D parametric design software programs widely used for product design, engineering, and manufacturing. It allows you to:

Design:

Create 3D models: Build accurate and detailed models of parts and assemblies using various features like extrudes, sweeps, fillets, and chamfers.

Parametric design: Modify any aspect of your design by simply changing the base features or dimensions, automatically updating the entire model. This saves time and ensures consistency.

Assembly building: Assemble parts into complex mechanisms and systems, checking for clearances and potential interference.

5.6. What Does SolidWorks Do ?

Simulation and analysis: Perform basic stress, thermal, and motion analysis to understand how your design will behave in real-world conditions.

Design for manufacturing (DFM): Incorporate manufacturing considerations into your design, making it easier and more cost-effective to produce.

SolidWorks Composer: Create technical illustrations and animations to document your design and instructions.

Collaboration tools: Share designs and revisions with other team members through cloud-based tools.

Product data management (PDM): Organize and manage design data throughout the product lifecycle.

Add-ins and customizations: Extend the functionality of SolidWorks with various add-ins and custom tools.

Improved design accuracy and efficiency: Parametric design reduces errors and rework, saving time and resources.

6. Materials and methods

The purpose of the design idea, motion generation mechanism, design process, and prototype execution is to demonstrate the efficacy of the evaluations. This article introduces forceps. Steel, aluminum and stainless spring steel were the materials we thought about using. We completed our task with these supplies. Using the Ansys and SolidWorks software, we chose these materials and created our designs and drawings on them.

6.1. Stainless Spring Steel (1.8159)

1.8159 is a designation for a specific steel grade known as 51CrV4. This steel is a high-grade alloy containing chromium (Cr), vanadium (V), and carbon (C). The designation "51" indicates it contains approximately 0.50% carbon. The addition of chromium and vanadium enhances the strength, toughness, and wear resistance of the steel, making it suitable for various applications, including springs, cutting tools, and high-stress components in mechanical engineering. Here are the main features and applications of stainless spring steel:

Key Features

Corrosion resistance: Stainless spring steel is highly resistant to corrosion, making it suitable for use in harsh environments including marine and chemical applications.

Elasticity: the material has a high resistance, thanks to which it recovers its original shape after deformation. This feature is necessary for springs and other components that are repeatedly loaded and unloaded.

Strength and Hardness: It offers a good balance between strength and hardness, ensuring durability and longevity in demanding applications.

Fatigue resistance: Steel can withstand cyclic loading without failure, which is crucial for components under repeated stress.

Applications Stainless spring steel is used in a variety of applications in various industries:

Automotive: Springs, retainers and fasteners that require both strength and corrosion resistance.

Aviation: high-quality springs and components that must withstand extreme conditions.

Medical Devices: Springs and wire forms used in surgical instruments and implants due to their biocompatibility and resistance to sterilization processes.

Marine: Parts exposed to sea water, such as cliffs, mountains and springs.

Industrial equipment: valves, actuators and other mechanisms that require reliable performance under cyclic loads.

Stainless spring steel is an important material in applications where high strength, ductility and corrosion resistance are required. Its versatile quality and features allow it to be used effectively in many demanding environments, making it a versatile and reliable choice for engineers and designers.

6.2. Aluminum

Aluminum is one of the materials that the project uses. a. Aluminum is utilized in a few unique locations and is now a part of our project. Aluminum has a matte silvery tone and is a soft, light metal. The thin coating of oxide that develops on it when it is exposed to air gives it this hue. Both non-toxic and non-magnetic aluminum exists. Sparks are not produced by it. The tensile strength of pure aluminum is about 49 MPa, but after alloying, it rises to 700 MPa. It has a density that is around one-third that of copper or steel. It is simple to manufacture, cast, and forge. Aluminum has also been included in this project because metal is frequently utilized in the medical industry.

6.3. Steel

Steel has become a valuable element in our project because of its versatility and longevity. Steel is an alloy made up of carbon and iron, with the carbon content typically ranging from 2.1% to 0.02%. Steel is categorized mostly based on the quantity of carbon in the alloy. Even though carbon is often used to alloy iron, other elements can also be employed, including magnesium, chromium, vanadium, and tungsten. Through their ability to stop the crystal lattices in iron atoms from sliding past one another, carbon and other elements function as hardening mediators. Hardness, ductility, and stress point in the final steel are all influenced by the varying concentrations of alloying elements in the steel as well as their forms (soluble elements, precipitation phase). Because of its durability, we considered utilizing steel for our project's arms.

6.4. Ni-Ti

Nickel titanium material is the last material alloy taken into consideration for this project. In intermetallic compounds known as nickel-titanium alloys, the atomic proportions of the elements titanium and nickel are either equal or nearly equivalent. In 1962, the nickel titanium alloy, or Ni Ti for short, was first discovered. The Nickel Titanium alloy was initially found by William James Buehler, a metallurgist at the US Naval Warfare Equipment Laboratory, and his associates. This alloy they found was given the name NITINOL. "Ni" stands for nickel, "Ti" for titanium, and "NOL" for "Naval Ordnance Laboratory" when referring to the word NITINOL. The decision was made to employ nickel titanium as the last material in this project. The SolidWorks platform was utilized to evaluate the characteristics of Nickel Titanium.

7. Current status and related studies

Many articles were examined while making this report. These articles are listed below. By reviewing the articles below, we examined what we could do differently. We designed the robotic arm we designed so that it can be bent in more axes than others, and we showed in the analysis section that it can be bent to other axes. In this way, more successful surgeries can be performed. A new design has been introduced to the world of robotics used in surgeries.

7.1. 3.5 mm compliant robotic surgical forceps with 4 DOF : design and performance evaluation D. S. V. Bandara, Ryu Nakadate, Murilo M. Marinho, Kanako Harada, Mamoru Mitsuishi & Jumpei Arata

The two primary features of this forceps are its four degrees of freedom (4 DOF) and 3.5 mm size. The authors describe the design aspects of the forceps in depth, emphasizing its compliance, which allows for flexibility and adaptability during surgical procedures. The forceps' compliance is crucial for navigating through intricate anatomical structures and ensuring precise manipulation. The report also includes a performance review of the robotic forceps, which most likely covers features like precision, reliability, and range of motion. This work contributes to the ongoing advancement of robotic surgery technology by introducing a compact, multifunctional surgical tool. By offering more precision and maneuverability in a variety of medical applications, such cooperative robotic forceps could enhance minimally invasive surgical techniques. The design presented in this article was attempted, but it was quickly apparent that it might be improved, so we concentrated on that aspect of the project.

The graphic displays the anticipated study to be conducted in this paper. It was determined to construct this design because the one presented in this article can only be twisted in one direction. Four components made up the exoskeleton in our design. The scissors at the end were bent to different axes each time we tugged these sections. The design was greatly aided by this article.. At the same time, what we saw in the analysis section was very helpful in analyzing our design. The figure below shows the design we made according to this article.

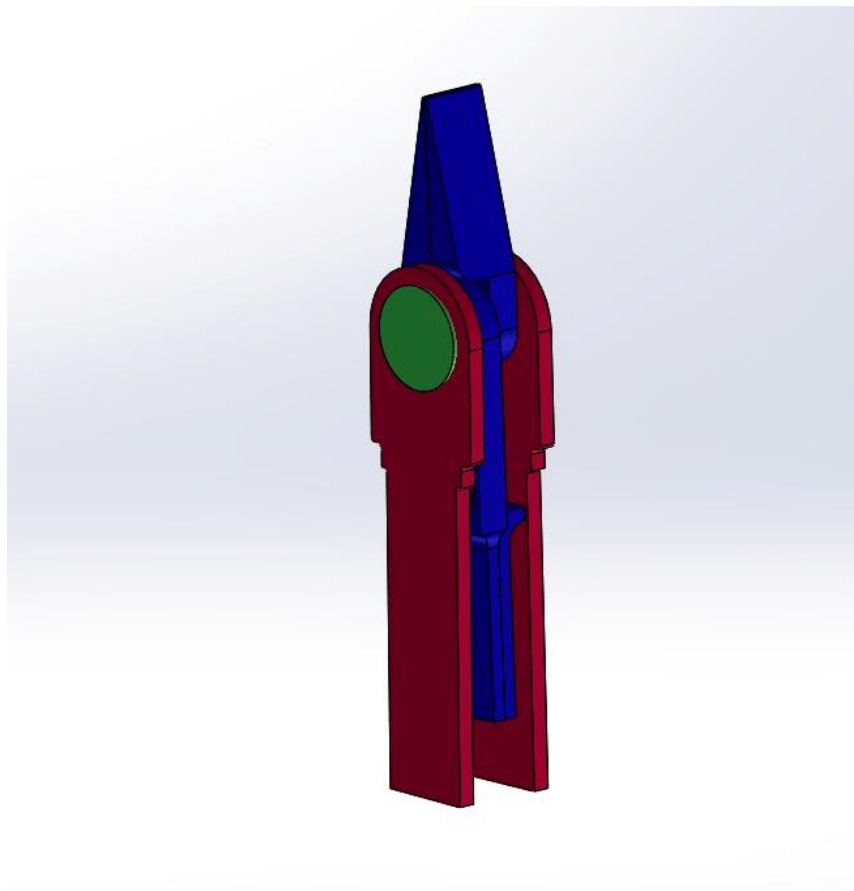


Figure 3: robotic surgical forceps with 4 DOF

7.2. Sensored Surgical Forceps for Robotically Assisted Minimally Invasive Surgery Authors: Kim, Uikyum; Kim, Yong Bum; So, Jinho; Seok, Dong-Yeop; Choi, Hyouk Ryeol

In the context of robotically aided minimally invasive surgery (MIS), the development and application of censored surgical forceps are covered in the paper "Censored Surgical Forceps for Robotically Assisted Minimally Invasive Surgery." The main objective is to improve precision and feedback during robot-assisted surgeries by integrating sensors into surgical tools, especially forceps. With the use of sensors, surgeons can more precisely monitor and control the delivered force, which improves the overall performance of robotic surgery. This article looks at the possible benefits of the technology, including increased safety, better surgical results, and a deeper comprehension of tissue interactions.

We want to make our movement in all 3 axes, as in this article. However, there are places in the design that we want to change. Therefore, a newer design was considered. At the same time, improvements were made in the design to make the movement of the scissors safer and more flexible.



Figure 4: Locations of force sensors on a surgical instrument. (a) The forceps composed of two jaws. (b) Teeth region and proximal region on a jaw.

7.3. Lyapunov-based bilateral teleoperation for surgical robotic forceps system with time varying delay Authors: Ishii, Chiharu; Mikami, Hiroyuki; Nishitani, Yosuke

They used the double-screw-drive forceps (DSD) approach in their creation. This strategy yielded significant benefits for sprains. This method was also considered and evaluated when developing our design and conducting our study. This article's primary focus is buckling. It works in part the way we would like. The usage of an enormous amount of parts is what makes it different. This design is not what we want in terms of part production and cost because of its small size. In addition to all of them, this essay gave us important ideas about bidirectional buckling. It was quite helpful in creating our layout. It also functioned as a model for the software required to guarantee the operation of the engines located at the rear.

They used the DSD (double-screw-drive forceps) technique in their design. This technique provided significant benefits in sprains. This technique was also considered and evaluated while making our design and performing our analyses.

This article focuses more on buckling. It works similar to what we want. However, the difference is that too many parts are used. This is a design we do not want, both in terms of cost and production of the part because it is small. In addition to all these, this article gave us very important ideas for bidirectional buckling. It was very helpful in creating our design. It also set an example for the software required for the correct operation of the engines mounted on the rear.

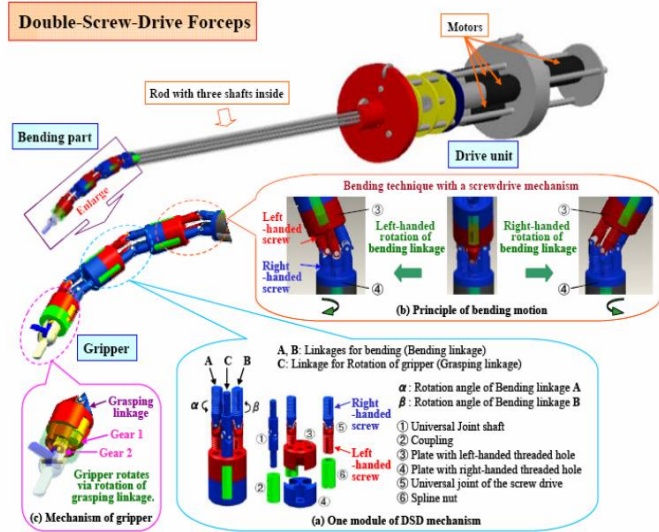


Figure 5: DSD forceps teleoperation system (see online version)

7.4. A New Type of Surgical Forceps Integrated with Three-Axial Force Sensor for Minimally Invasive Robotic Surgery

Authors: Kim, Uikyung; Kim, Yong Bum; Seok, Dong-Yeop; So, Jinho; Choi, Hyouk Ryeol

A novel kind of surgical forceps with a three-axial force sensor for robotic minimally invasive surgery is presented in the paper. This state-of-the-art surgical instrument features two grippers, each equipped with a capacitive force sensing three-axial force sensor. Because of their special design, surgical grippers can take precise force measurements without losing their original shape. Notably, it is simpler to detect palpation at the gripper's edge or rear since the force sensors are positioned distally on the gripper's tip. The principles of three-axial force sensing, the complexities of the design, and the potential benefits of this integration for enhanced precision and feedback in minimally invasive robotic surgery are covered in this work.

This article was designed to be able to move in 3 axes as we wanted. However, since its design was not what we thought it would be, only its rotation in three axes was taken into account. At the same time, in this article, we do not want the movements to be made with electrical energy. Our robotic forceps is designed to move in two axes and is a mechanical arm. It is designed to move with power.



Figure 6: Actual picture of the forceps composing the two sensorized gripper.

7.5. Force Sensor Integrated Surgical Forceps for Minimally Invasive Robotic Surgery Authors : Kim, Uikyum; Lee, Dong-Hyuk; Yoon, Woon Jong; Hannaford, Blake; Choi, Hyouk Ryeol

The creation of force sensor-integrated surgical forceps for use in minimally invasive robotic surgery is covered in the article. Two grippers on these force sensor-integrated forceps are outfitted with three-axial force sensors that use a capacitive-type sensing technique. Precise force measurement at various points is made possible by the sensors on the gripper's tip being strategically placed. The paper highlights the fundamentals of three-axial force sensing and discusses how it might improve surgical feedback and precision. All things considered, the addition of force sensors to these surgical forceps is seen as a major development toward enhancing safety and control in minimally invasive robotic surgery.

This article contains a design without using buckling. With this design, the scissor tips can move in the east-west directions, but it will take up a lot of space while moving towards the north and south directions. There is a high probability of harming the patient in its movements. However, this design is also very useful. In our design, it prevents spraining while moving towards the north and south directions. In this way, there will be no restriction of movement during the operation and the surgeries will be more successful.

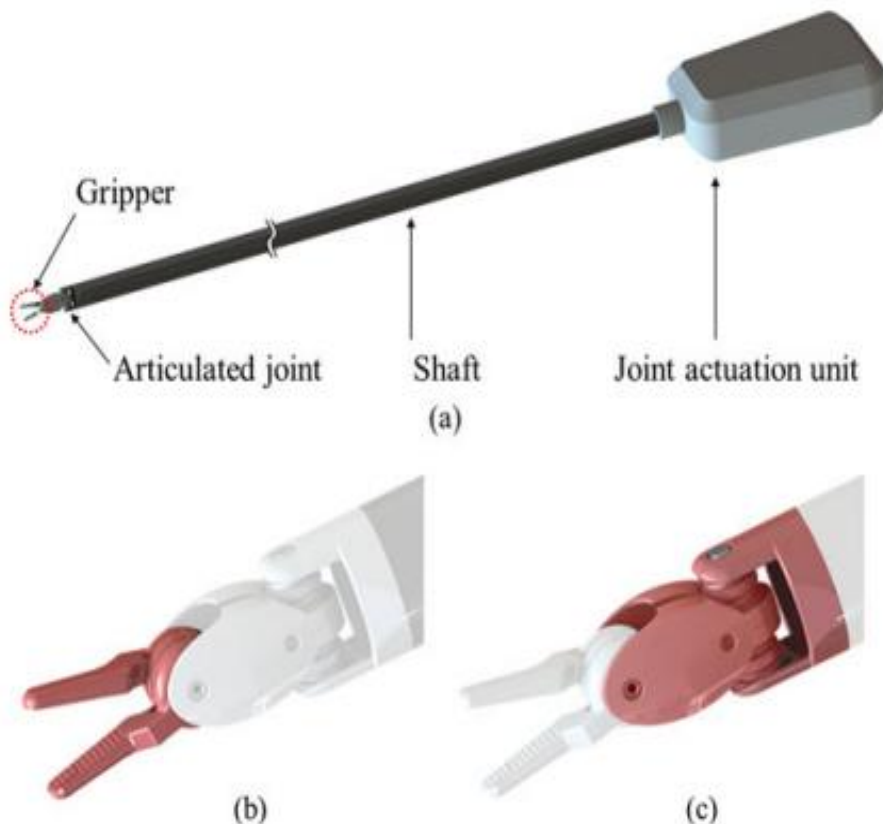


Figure 7: (a) Entire surgical instrument. (b) Three-dimensional model of gripper. (c) Three-dimensional model of articulated joint.

7.6. Meta-analysis of observational studies on the safety and effectiveness of robotic gynaecological surgery Authors:M. Reza; S. Maeso; J. A. Blasco; E. AndradasM. Reza; S. Maeso; J. A. Blasco; E. Andradas

A meta-analysis of observational studies examining the safety and effectiveness of robotic gynecological surgery reveals encouraging findings. The review, which included numerous trial findings, found that the safety profiles and efficacy of robotically assisted gynecological procedures were comparable to those of more traditional methods. Significant research demonstrates that compared to traditional techniques, robotic surgery has fewer problems, shorter hospital stays, and quicker recovery times. Although these results are encouraging, more randomized controlled trials are needed to fully understand the benefits and potential risks of robotic gynecological surgery.

7.7. Transanal specimen extraction in robotic rectal cancer surgery Authors:J. Kang; B. S. Min; H. Hur; N. K. Kim; K. Y. Lee

A robotic rectal cancer surgery technique called transitional specimen extraction involves cutting out the tumor and surrounding tissue through the anus. When combined with robotic help, this technology allows for less invasive surgeries and may reduce the need for larger incisions. Studies show that robotic rectal cancer surgery with transitional specimen extraction produces superior cosmetic outcomes, less pain after surgery, and a shorter recovery period than open procedures. Additionally, it might lead to fewer issues and shorter hospital stays. Although promising, more research and surgical experience are required to ascertain the long-term efficacy and safety of this approach.

8. Design

Design is the process of planning and creating an object, process, service or system for a specific purpose. Design covers a wide range of disciplines and takes into account many factors such as aesthetics, functionality, ergonomics, user experience, durability and manufacturing. The key elements of design are needs and goals, creativity and innovation, aesthetics, functionality, user experience (UX) and sustainable development. Needs and objectives are the point at which the design process begins to address a specific need or solve a problem, where designers gather information about the target audience and the purpose of the design. Creativity and innovation are the main components of design in the development of creative ideas and innovative solutions. Aesthetics is an important part where visual appeal as well as aesthetic elements and elements such as color, shape, texture, and layout are taken into consideration. Functionality means that the design must be functional and effectively meet the identified need. User experience (UX) aims to improve user interaction and design experience. However, the sense of responsibility highlights the development of environmentally friendly and sustainable solutions as an important part of modern design. In this context, we designed our design by paying attention to these points. However, our main goal is to create a design that can work in a healthy way.

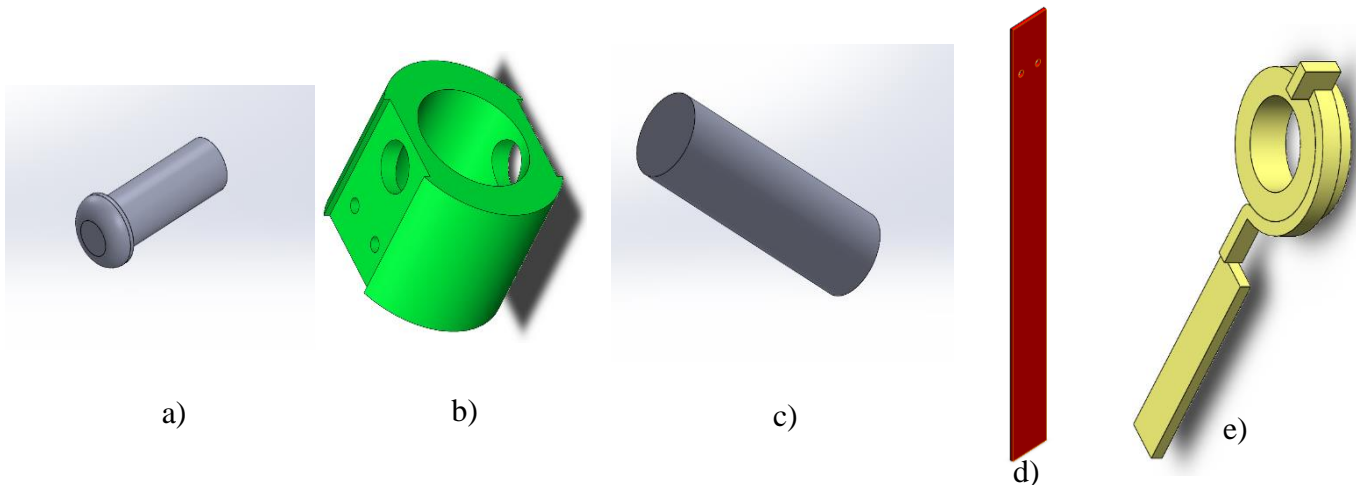


Figure 8: a)M5 screw b)Cylinder(head) c)pin d)Stainless spring steel e)scissors with spring

First of all, previously written articles on design were examined and a literature review was made. Then, the design in this article was tested by taking an article as an example. It was discussed how the design could be improved better. For this, many trials and errors were made. In order for the design to have a more mobile and simpler structure. Many designs were tried. As a result of the trials, the design shown below was decided.

This design we made consists of five parts. First of all, the head part was designed as a cylinder and stainless spring steels were designed to enter the interior of this cylinder. However, this design was abandoned because it required too much cost and effort in the production part. It was decided to make a new design. Stainless steel was placed on the sides of the cylinder. A slot was opened, large enough to accommodate the spring steel. In this way, production costs were avoided and installation was made easier. The slot for the shaft was also opened in the size of the shaft where the scissors would be fixed. This design was drawn and produced on the CNC machine.

Screw slots were opened to mount the stainless spring steels to the cylinder. In order to make the design healthier and more useful, the outer surface of the stainless spring steels was given a circular shape, like a cylinder. In this way, there will be no sharp surface during the surgery and damage to the tissues will be avoided. This is the main reason why we use the cylinder shape. Since there will be no corner points in the design, any tissue damage or damage to the tissue is prevented.

With the designs we have made so far, we have ensured that the product bends in the x axis. In addition, its movement in the y axis had to be ensured. For this, it was decided that this movement could be achieved with scissors, after being considered during the design process. This movement can be achieved as an alternative by using a second cylinder. Likewise, the first one was considered. By mounting the second cylinder on the y axis in the same way that the cylinder is mounted, the movement on the y axis can be achieved with the second cylinder.

With the movement of the motors under the scissors, movement in the other direction was ensured, and with these movements, the scissors were opened and closed. With the help of the motors, when we pushed one of the scissors and pulled the other, their rotation was ensured. It was mounted on the shaft with the help of a ring. In this way, the movement was ensured easily. The scissors were designed with stainless spring steel so that they can move more easily underneath.

During the assembly, the shaft was first placed in the slot we opened for the shaft. Then, the stainless spring steels on the outer surface of the cylinder were mounted using M5 screws. In this way, the shaft was prevented from moving axially, but there was no obstacle to its rotational movement. After the assembly of the shaft was completed, the scissors were connected to the shaft. After these stages were completed, the assembly of the stainless spring

steel on the other side was completed with an M5 screw and the construction phase of the product we designed was completed.

Finally, this design process we made was carried out together with the production process. Because the design had to be constantly changed due to problems in production. Many changes were made in the design in order to ensure a more reliable installation on the engines. As a result of many articles and studies we read and researched, this design was decided. The experiments and analysis were carried out. It was seen that the design was successful in some parts.

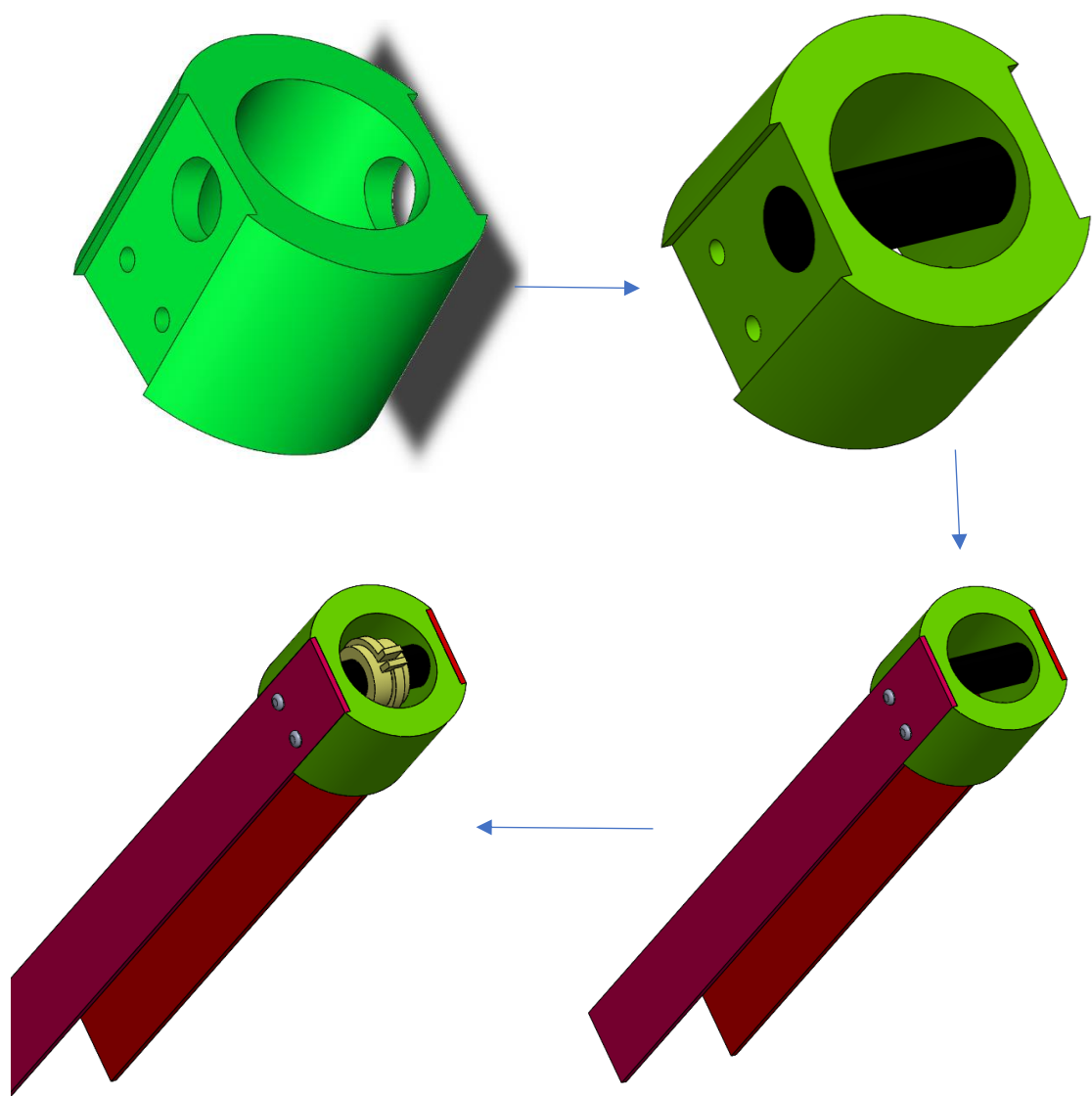


Figure 9: Assembly stages

9. Motion

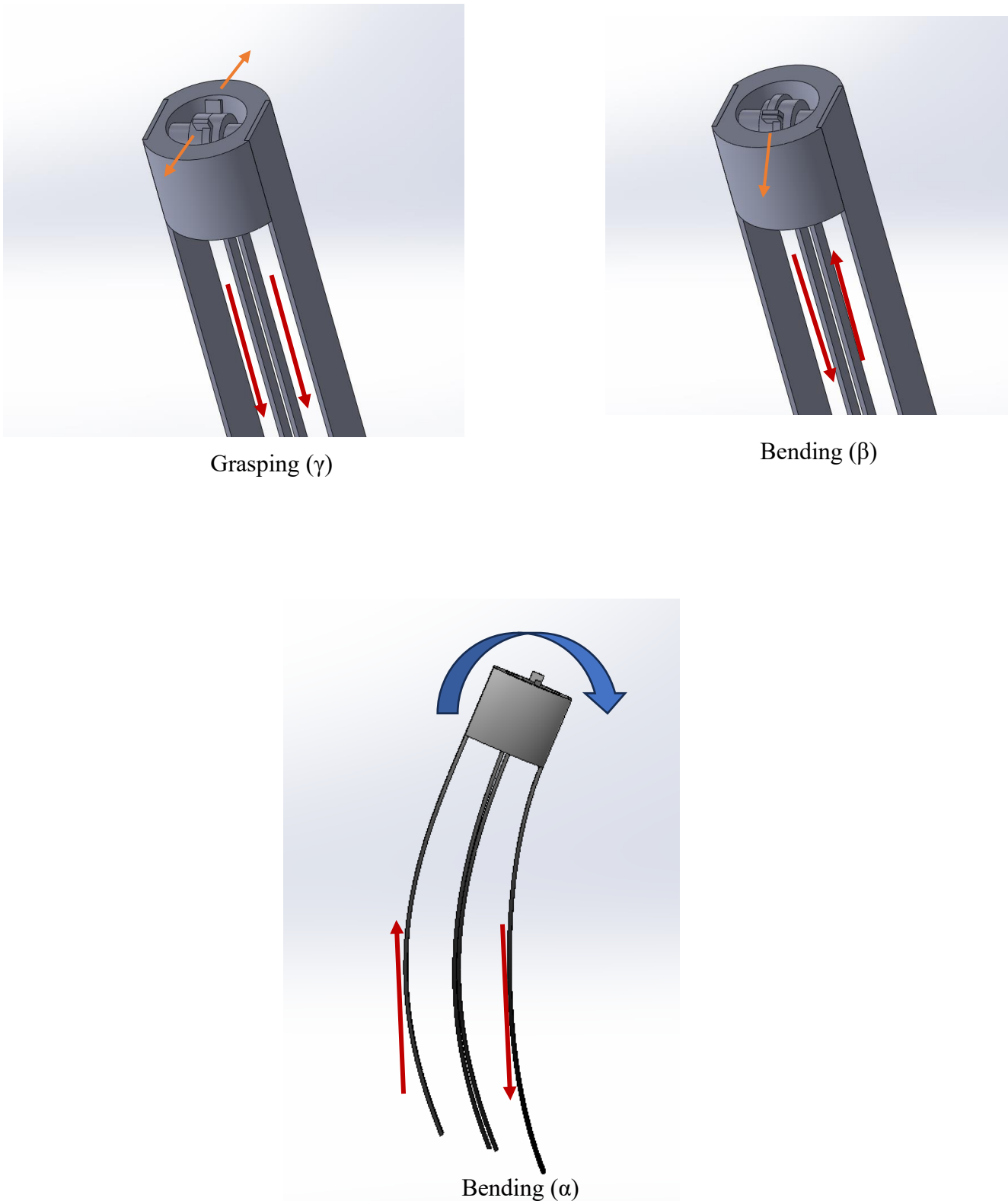


Figure 10: movement of design

10. Kinematic Model

10.1. For Bending (α)

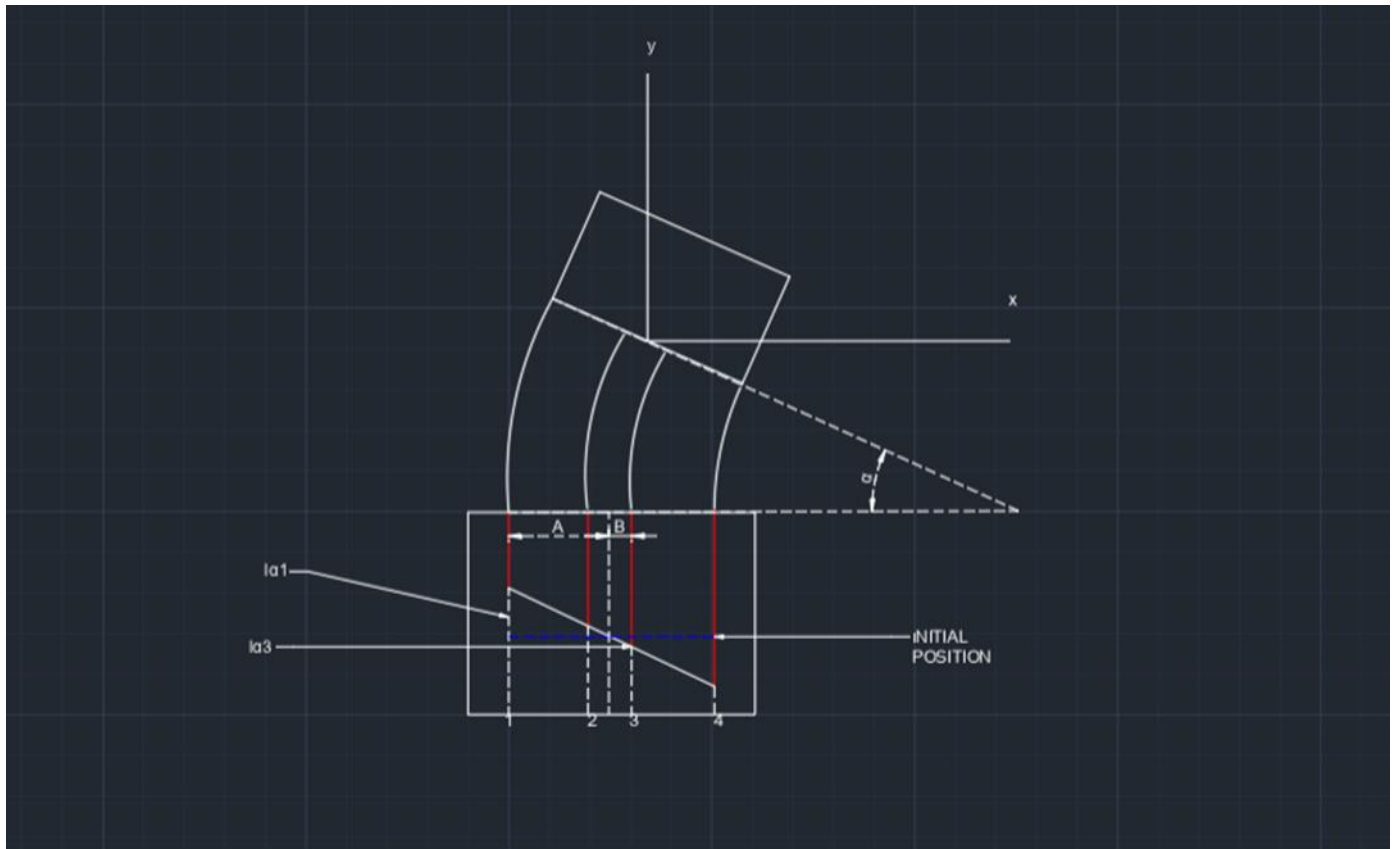


Figure 11: Overview of the kinematic structure α bending

In figure illustrates the details of the defined parameters for the kinematic model of the proposed design. Here, the curvature of the springs during motion generation was assumed to be circular arcs. Furthermore, the springs were assumed to behave linearly and symmetrically in both directions. In Figure the angles related to the two bending motions are denoted by α and β . Grasping is denoted by γ .

In this kinematic model, we used the linear displacement of our springs and our constants to obtain the α angle. Distance A represents the distance between spring 1 and the center line. Distance B represents the distance of one of the springs of the scissors from the center.

We obtained the following formulas with the geometric solutions we made. The four rigid links 1-4 were displaced by distance L_{a1} , L_{a2} , L_{a3} and L_{a4} , respectively, from the initial position to generate an α° angle of the α bending motion. Thus,

Inverse

$$La_1 = A \times \tan \alpha \quad (1)$$

$$La_2 = -A \times \tan \alpha \quad (2)$$

$$La_3 = B \times \tan \alpha \quad (3)$$

$$La_4 = -B \times \tan \alpha \quad (4)$$

Forward

$$\alpha = \tan^{-1} \frac{L_{\alpha_1}}{A} \quad (5)$$

$$\alpha = \tan^{-1} \left(-\frac{L_{\alpha_2}}{A} \right) \quad (6)$$

$$\alpha = \tan^{-1} \left(\frac{L_{\alpha_3}}{B} \right) \quad (7)$$

$$\alpha = \tan^{-1} \left(-\frac{L_{\alpha_4}}{B} \right) \quad (8)$$

10.2. For Bending (β)

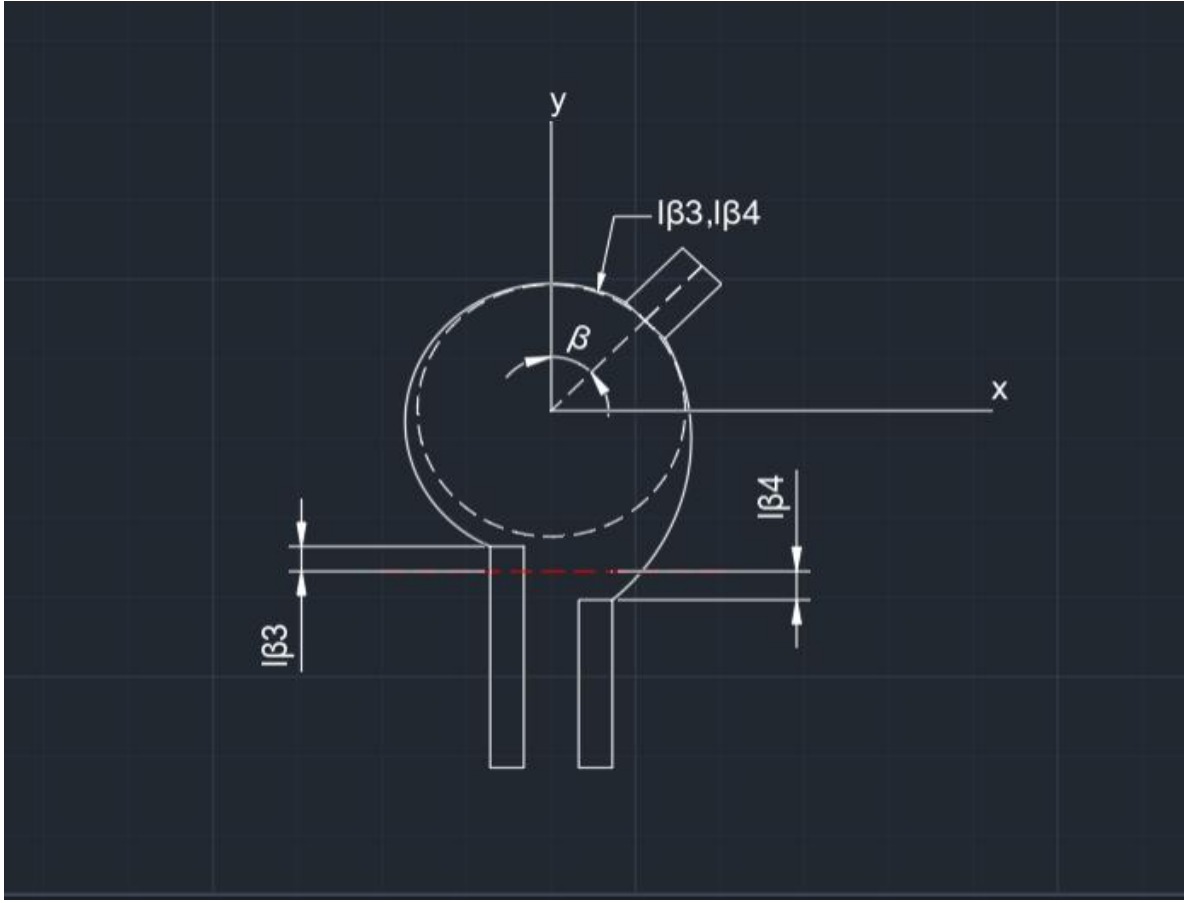


Figure 12: Overview of the kinematic structure β bending

To achieve bending in the scissors, we need to move one of the scissor springs linearly downwards while the other moves linearly upwards. As a result of this movement, the bending angle was found by taking into account the distances to the starting line.

Thus, for β bending, links 3 and 4 were, respectively, displaced by distances L_{β_3} and L_{β_4} from the initial position to generate β° angle. Thus,

Inverse

$$L_{\beta_3} = (\beta/360) * 2\pi r \quad (9)$$

$$L_{\beta_4} = -(\beta/360) * 2\pi r \quad (10)$$

Forward

$$\beta = \frac{L_{\beta_3} * 360}{2\pi r} \quad (11)$$

$$\beta = -\frac{L_{\beta_4} * 360}{2\pi r} \quad (12)$$

10.3. For Grasping (γ)

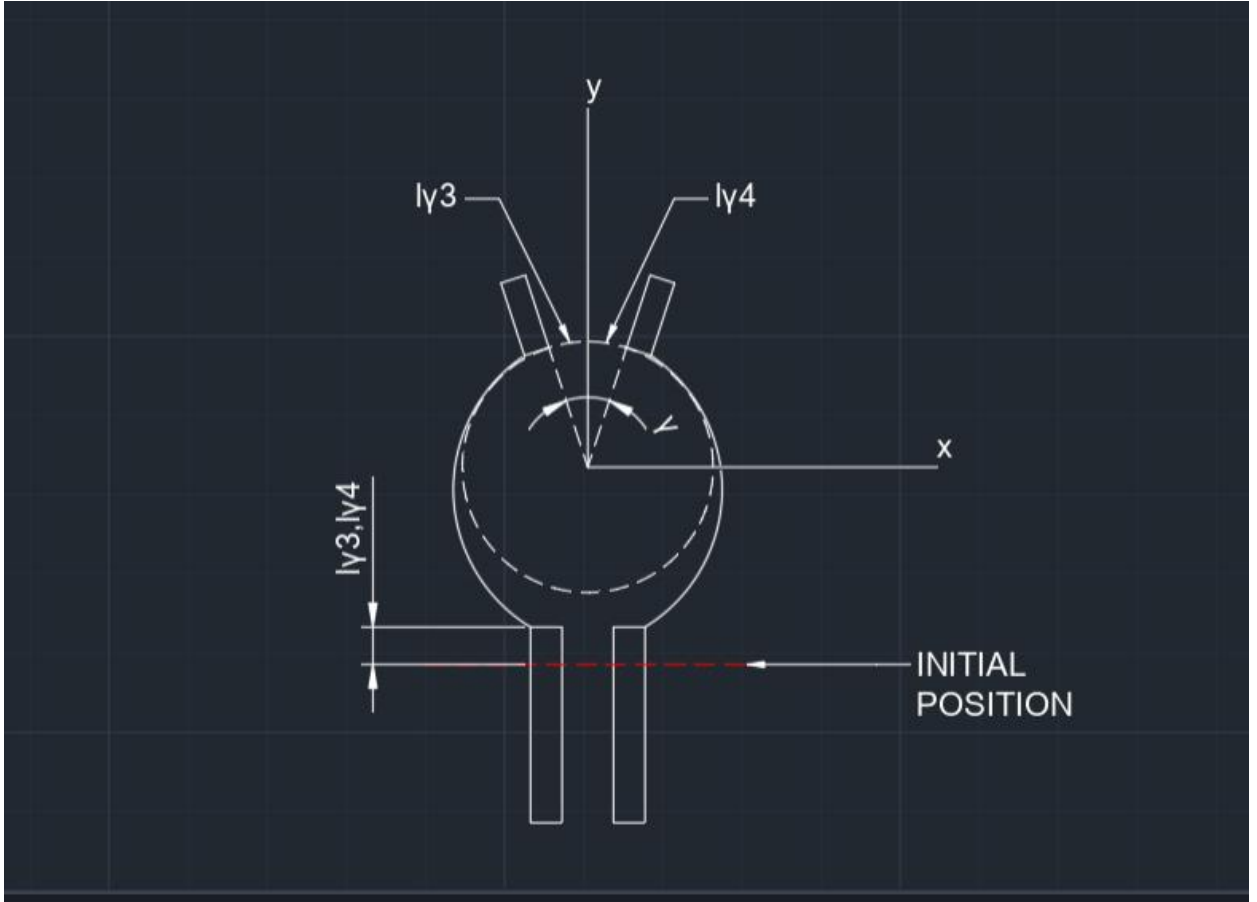


Figure 13: Overview of the kinematic structure γ , grasping.

Inverse

$$L\gamma_3 = (\gamma/720) * 2\pi r \quad (13)$$

$$L\gamma_4 = -(\gamma/720) * 2\pi r \quad (14)$$

Forward

$$\gamma = \frac{L\gamma_3 * 720}{2\pi r} \quad (15)$$

$$\gamma = -\frac{L\gamma_4 * 720}{2\pi r} \quad (16)$$

These equations show the formulas for the displacement that occurs when the scissors are opened and closed. How far the scissor springs moved from the starting point was used to determine the grasping angle of the scissors.

In the table below, the displacement amounts that occur according to the given angles are given. Thanks to these displacement amounts, the total displacement is learned

10.4. Overall kinematic model

$$L1 = A \times \tan\alpha \quad (17)$$

$$L2 = -A \times \tan\alpha \quad (18)$$

$$L3 = B \times \tan\alpha + (\beta/360) * 2\pi r + (\gamma/720) * 2\pi r \quad (19)$$

$$L4 = -(B \times \tan\alpha + (\beta/360) * 2\pi r + (\gamma/720) * 2\pi r) \quad (20)$$

Table 1: Table of linear motion length based on degree values

$\alpha(\text{degree})$	$\beta(\text{degree})$	$\gamma(\text{degree})$	$L_{1a}(\text{mm})$	$L_{2a}(\text{mm})$	$L_{3a}(\text{mm})$	$L_{4a}(\text{mm})$	$L_{3\beta}(\text{mm})$	$L_{3\gamma}(\text{mm})$	$L_{4\beta}(\text{mm})$	$L_{4\gamma}(\text{mm})$
1	1	1	0,262	-0,262	0,009	-0,009	0,087	0,044	-0,087	0,044
2	2	2	0,524	-0,524	0,017	-0,017	0,175	0,087	-0,175	0,087
3	3	3	0,786	-0,786	0,026	-0,026	0,262	0,131	-0,262	0,131
4	4	4	1,049	-1,049	0,035	-0,035	0,349	0,175	-0,349	0,175
5	5	5	1,312	-1,312	0,044	-0,044	0,436	0,218	-0,436	0,218
6	6	6	1,577	-1,577	0,053	-0,053	0,524	0,262	-0,524	0,262
7	7	7	1,842	-1,842	0,061	-0,061	0,611	0,305	-0,611	0,305
8	8	8	2,108	-2,108	0,070	-0,070	0,698	0,349	-0,698	0,349
9	9	9	2,376	-2,376	0,079	-0,079	0,785	0,393	-0,785	0,393
10	10	10	2,645	-2,645	0,088	-0,088	0,873	0,436	-0,873	0,436
11	11	11	2,916	-2,916	0,097	-0,097	0,960	0,480	-0,960	0,480
12	12	12	3,188	-3,188	0,106	-0,106	1,047	0,524	-1,047	0,524
13	13	13	3,463	-3,463	0,115	-0,115	1,134	0,567	-1,134	0,567
14	14	14	3,740	-3,740	0,125	-0,125	1,222	0,611	-1,222	0,611
15	15	15	4,019	-4,019	0,134	-0,134	1,309	0,654	-1,309	0,654
16	16	16	4,301	-4,301	0,143	-0,143	1,396	0,698	-1,396	0,698
17	17	17	4,586	-4,586	0,153	-0,153	1,484	0,742	-1,484	0,742
18	18	18	4,874	-4,874	0,162	-0,162	1,571	0,785	-1,571	0,785
19	19	19	5,165	-5,165	0,172	-0,172	1,658	0,829	-1,658	0,829
20	20	20	5,460	-5,460	0,182	-0,182	1,745	0,873	-1,745	0,873
21	21	21	5,758	-5,758	0,192	-0,192	1,833	0,916	-1,833	0,916
22	22	22	6,060	-6,060	0,202	-0,202	1,920	0,960	-1,920	0,960
23	23	23	6,367	-6,367	0,212	-0,212	2,007	1,004	-2,007	1,004
24	24	24	6,678	-6,678	0,223	-0,223	2,094	1,047	-2,094	1,047
25	25	25	6,995	-6,995	0,233	-0,233	2,182	1,091	-2,182	1,091
26	26	26	7,316	-7,316	0,244	-0,244	2,269	1,134	-2,269	1,134
27	27	27	7,643	-7,643	0,255	-0,255	2,356	1,178	-2,356	1,178
28	28	28	7,976	-7,976	0,266	-0,266	2,443	1,222	-2,443	1,222
29	29	29	8,315	-8,315	0,277	-0,277	2,531	1,265	-2,531	1,265
30	30	30	8,660	-8,660	0,289	-0,289	2,618	1,309	-2,618	1,309

11. Finite Element Analysis

In the section dedicated to finite element analysis, we embarked on a comprehensive examination of our robotic arm's structural integrity, aiming to understand its endurance under various operational conditions. This involved a multifaceted approach where we delved into assessing its resilience, identifying its workspaces, and determining the requisite forces and displacements to attain specific angular positions.

Our analyses encompassed a diverse array of scenarios, encompassing a spectrum of movements and stressors representative of real-world applications. To ensure the arm's ability to maneuver as required, we relied on kinematic analysis, a crucial tool that enabled us to predict the arm's behavior across different orientations.

Central to our analyses was the characterization of the material used in our robotic arm – stainless spring steel (1.8159, 51CrV4). By defining its properties within our simulations, we could accurately model its behavior under various loads and environmental conditions.

Through rigorous computations and simulations, we derived a set of formulas that guided us in determining the forces and displacements necessary for the robotic arm to achieve desired angles and positions. These calculations formed the cornerstone of our strategy to optimize the arm's performance and ensure its reliability in practical settings.

11.1. Material properties(Stainless Spring Steel (1.8159, 51CrV4))

Yielding strength of stainless spring steel = $7 \times 10^8 \text{ N/m}^2$

Tensile strength = $9 \times 10^8 \text{ N/m}^2$

Elastic modulus = $2.1 \times 10^{11} \text{ N/m}^2$

Yielding strength of Ni-Ti = $4 \times 10^8 \text{ N/m}^2$

11.2. For $\alpha = 15$ degree

$$La_1 = 4 \text{ mm } F = 5.1 \text{ N}$$

$$La_2 = -4 \text{ mm } F = 6.5 \text{ N}$$

$$La_3 = 0.14 \text{ mm } F = 4.2 \text{ N}$$

$$La_4 = -0.14 \text{ mm } F = 2.9 \text{ N}$$

In our initial analysis, we aimed to bend our robotic surgical arm by 15 degrees along the x and y axes. To achieve this, we utilized the formulas from our kinematic model to determine how much displacement each spring arm required. At the conclusion of the analysis, we observed and reported the von Mises stress levels and displacements obtained. Additionally, we investigated how much force would be required to apply the necessary displacements to the springs.

The forces that must be applied to obtain the displacement values seen in the equations have been found in the finite element analysis. It is seen that these forces change for each angle. When we apply the forces at the right rate, we will obtain bending according to the yield strength value of the material. When the determined forces are applied to obtain the desired angle, the displacements that must be given to the springs are obtained. As a result of the analysis made for 15 degrees, the force values were reached. The same application was made for other angle values and the force values obtained as a result of the analysis are shown.

$$A = 15 \text{ mm } B = 0.5 \text{ mm}$$

$$La_1 = A \times \tan \alpha$$

$$La_1 = 15 \text{ mm} \times \tan 15 = 4 \text{ mm}$$

$$La_2 = -La_1 = -4 \text{ mm}$$

$$La_3 = B \times \tan \alpha = 0.14 \text{ mm} = -La_4$$



Figure 14:a and b) Analysis for 15 degrees c) Von mises values for 15 degrees d) Distance values for 15 degrees e) estrn values for 15 degrees

11.3. For $\alpha = 30$ degree

For

$$\alpha = 30^\circ$$

$$L\alpha 1 = 8.65 \text{ mm } F = 10.4 \text{ N}$$

$$L\alpha 2 = -8.65 \text{ mm } F = 16.1 \text{ N}$$

$$L\alpha 3 = 0.31 \text{ mm } F = 8.2 \text{ N}$$

$$L\alpha 4 = -0.31 \text{ mm } F = 5.7 \text{ N}$$

Analogically, we performed a bending operation on our surgical robot arm, flexing it by 30 degrees individually along both the x and y axes. Employing our kinematic model, we calculated and executed these alterations. Upon reaching the 30-degree bend, we determined that our von Mises stress neared the brink of yielding strength. This observation implied that further displacement could induce material deformation. Consequently, based on the analysis, we determined the requisite force magnitude for these displacements and took necessary precautions to ensure the safe continuation of the operation.

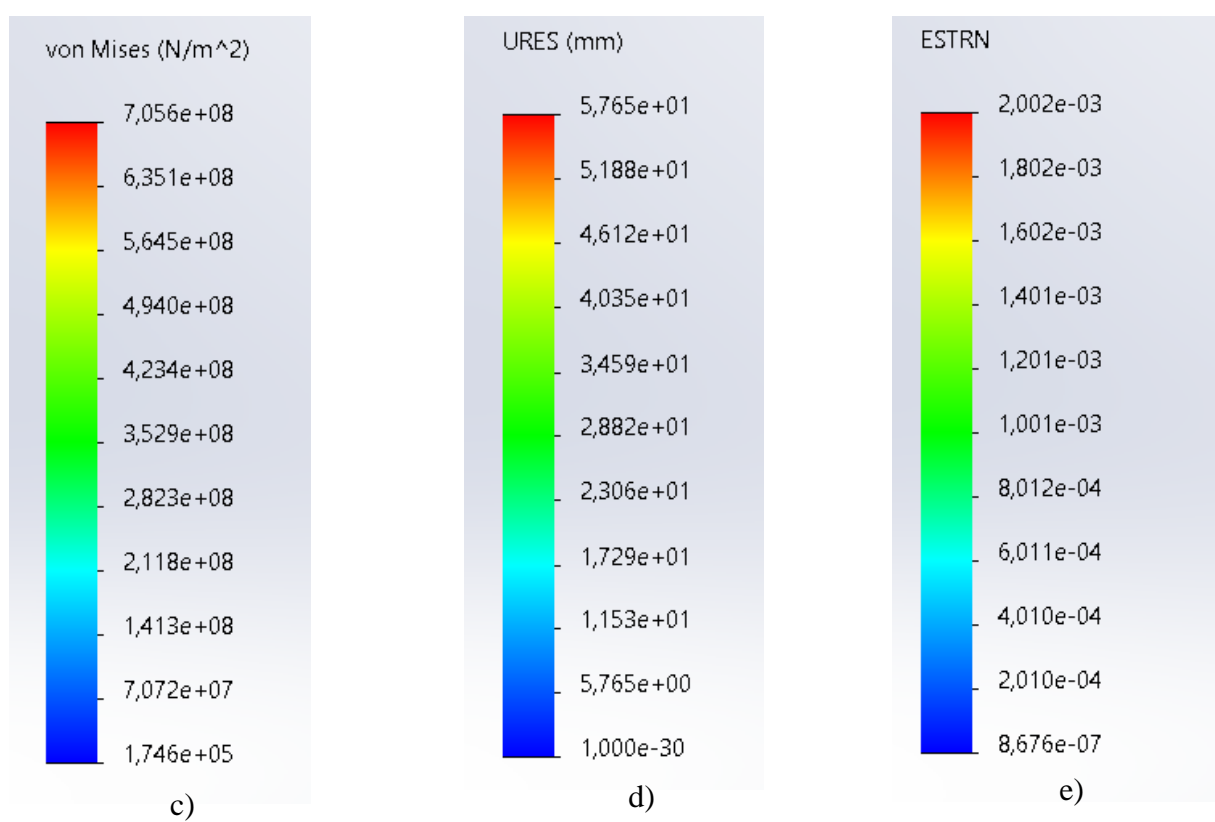
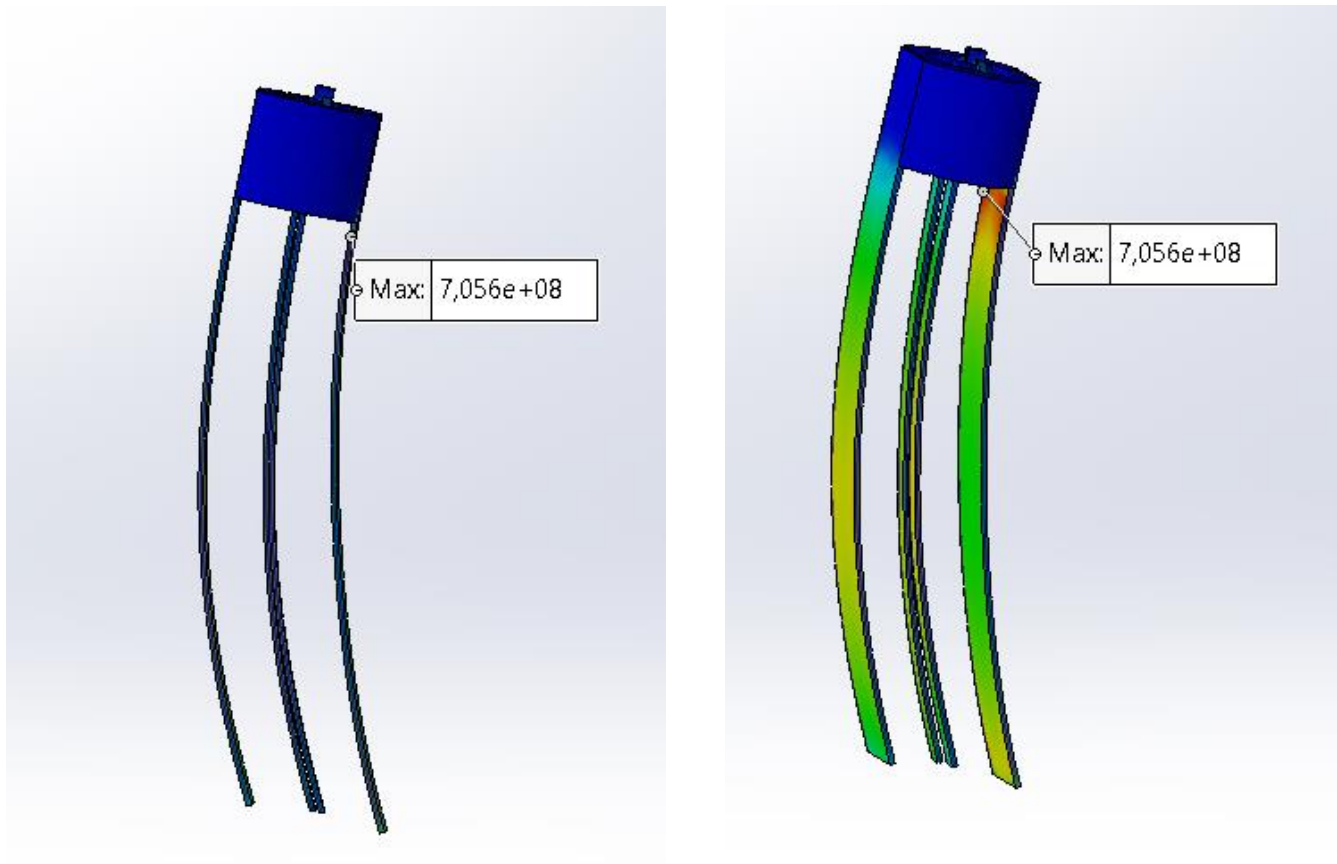


Figure 15: a and b) Analysis for 30 degrees c) Von mises values for 30 degrees d) Distance values for 30 degrees e) estrn values for 30 degrees

11.4. For $\alpha = 45$ degree

$$\alpha = 45^\circ$$

$$L\alpha_1 = 15 \text{ mm } F = 20.3 \text{ N}$$

$$L\alpha_2 = -15 \text{ mm } F = 24.5 \text{ N}$$

$$L\alpha_3 = 0.52 \text{ mm } F = 16.2 \text{ N}$$

$$L\alpha_4 = -0.52 \text{ mm } F = 12.8 \text{ N}$$

In our third analysis, we conducted a bending operation on our robotic surgical arm, flexing it by 45 degrees along both the x and y axes. Leveraging the capabilities of our kinematic model, we meticulously computed the displacements required to achieve this specific bend. Upon thorough examination of the analysis outcomes, we noted a considerable disparity between the von Mises stress and the yielding strength of our material. This discrepancy signaled that the applied displacement could potentially result in material deformations. Consequently, we gleaned valuable insights into the potential consequences of such displacement applications on our material integrity, informing our future operational strategies and material selection processes.

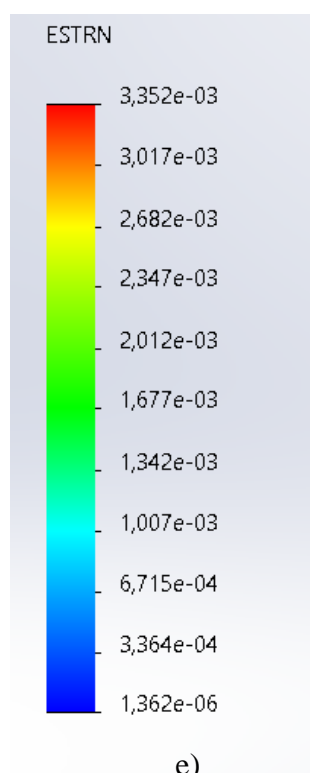
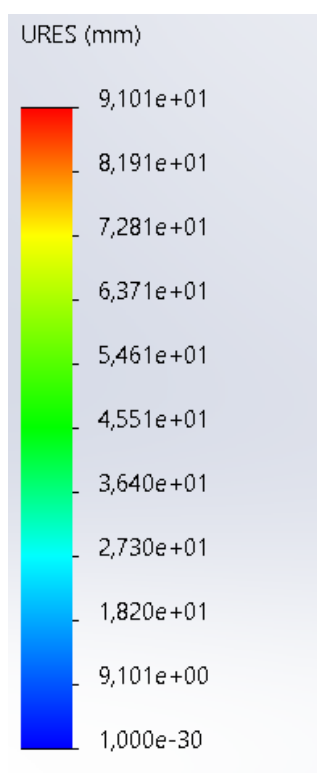
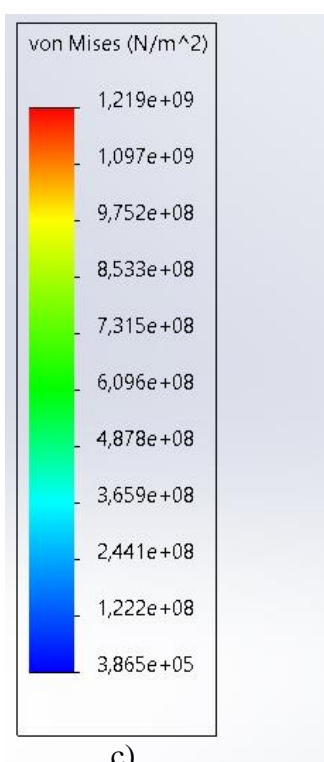
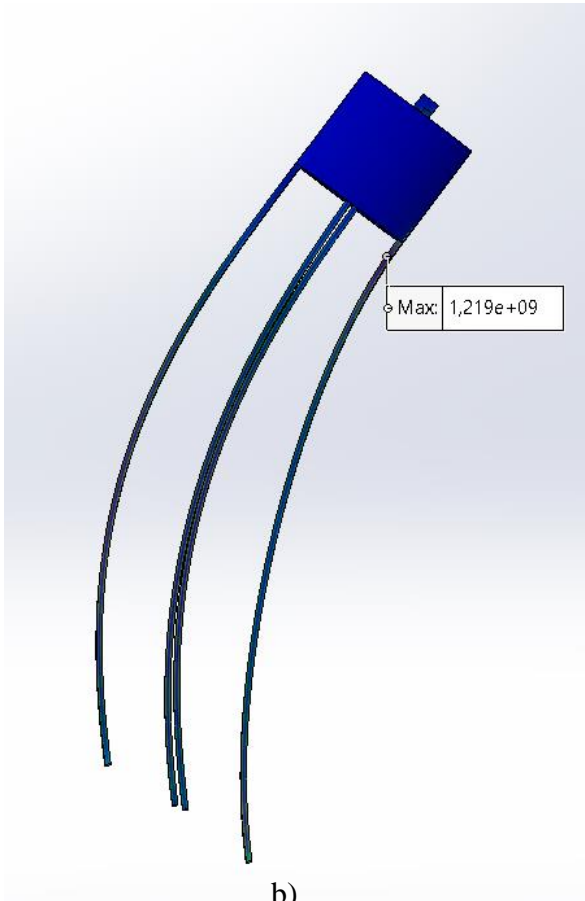
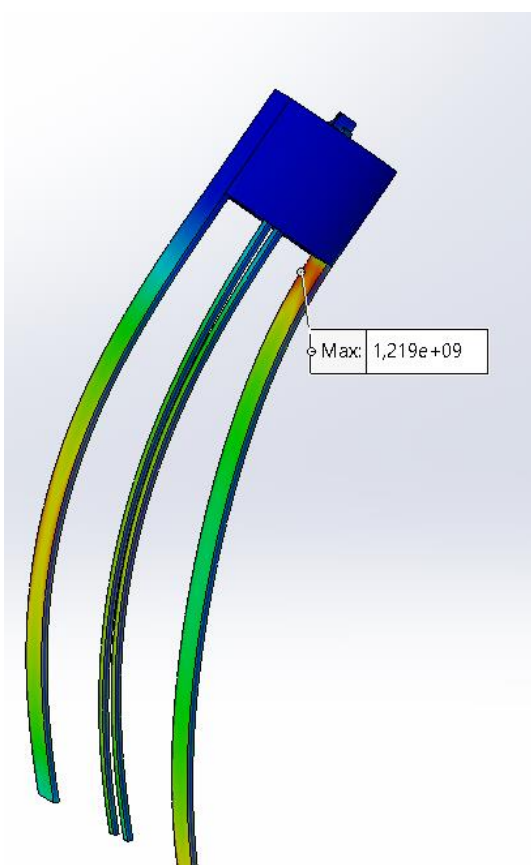


Figure 16: a and b) Analysis for 45 degrees c) Von mises values for 45 degrees d) Distance values for 45 degrees e) estrn values for 45 degrees

11.5. For $\alpha = 15^\circ$; $\gamma = 15^\circ$

$$\alpha = 15^\circ : \gamma = 15^\circ$$

$$L\alpha 1 = 8.65 \text{ mm } F = 30.2 \text{ N}$$

$$L\alpha 2 = -8.65 \text{ mm } F = 35.4 \text{ N}$$

$$L\alpha 3 = 1.9 \text{ mm } F = 24.8 \text{ N}$$

$$L\alpha 4 = 1.25 \text{ mm } F = 19.5 \text{ N}$$

In our fourth analysis, we embarked on a comprehensive exploration by subjecting our material to dual manipulations: a 15-degree bend along both the x and y axes and a concurrent 15-degree opening of our shears. This intricate investigation unearthed a significant revelation: the simultaneous execution of these movements led to a notably accelerated escalation in von Mises stress, breaching the yielding strength threshold of our material. To facilitate analyses at desired degrees, we meticulously computed and enacted the requisite displacements within our kinematic model. Furthermore, we delved into scrutinizing the requisite force magnitude necessary to induce the stipulated displacements, illuminating crucial insights for operational optimization and material resilience enhancement.

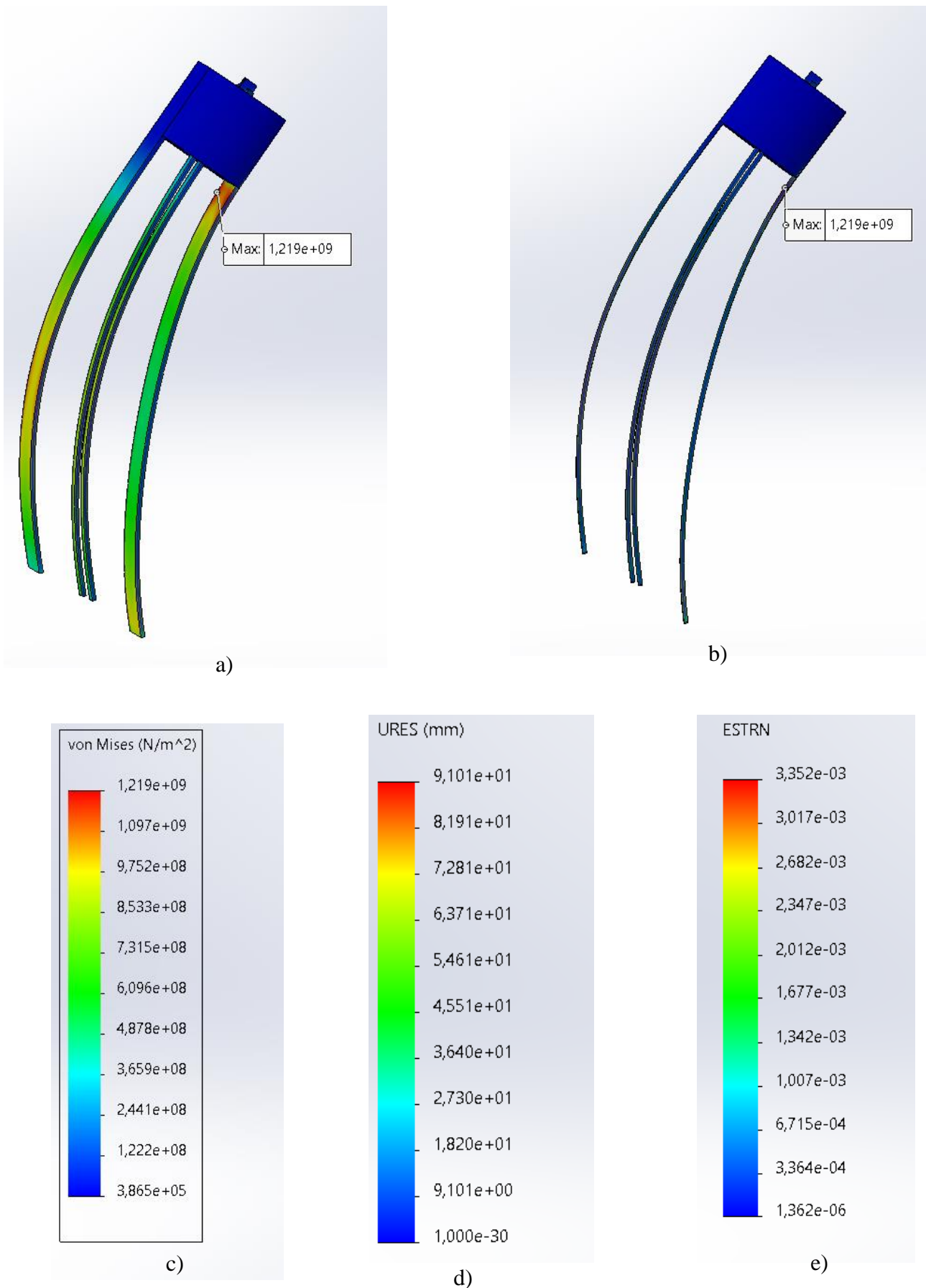


Figure 17: a and b) Analysis for 15 degrees c) Von mises values for 15 degrees d) Distance values for 15 degrees e) estrn values for 15 degrees

11.6. For $\alpha = 15^\circ$; $\gamma = 15^\circ$; $\beta = 15^\circ$

$$L_1 = 4,019 \text{ mm} \quad F = N$$

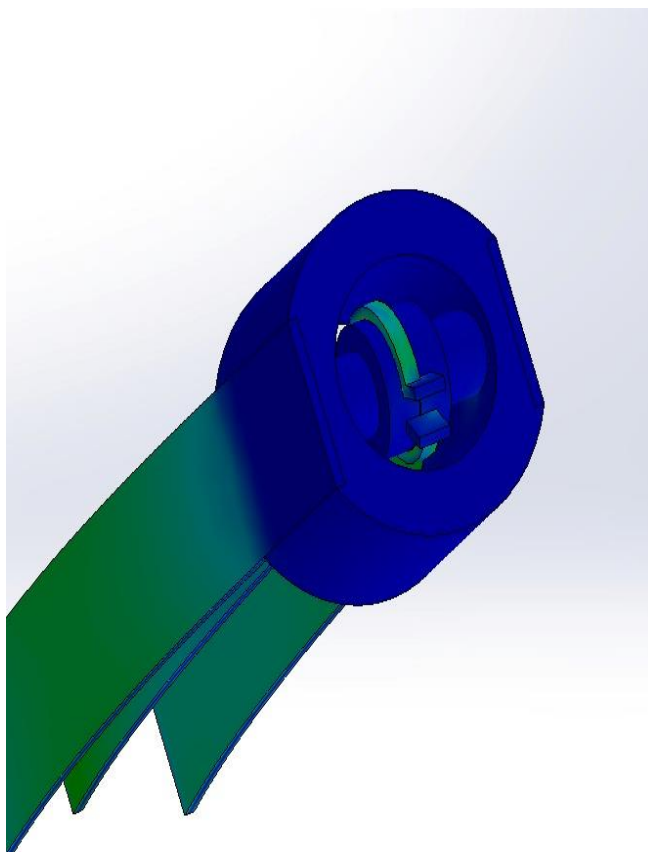
$$L_2 = -4,019 \text{ mm} \quad F = 48,8 \text{ N}$$

$$L_3 = 2,097 \text{ mm} \quad F = 21 \text{ N}$$

$$L_4 = 0,788 \text{ mm} \quad F = 20 \text{ N}$$

In our analysis, we aimed to utilize all three angles - alpha, beta, and gamma - specified in our kinematic model. We set each angle to 15 degrees and aimed to examine the structural behavior under these conditions. Throughout our analysis, we observed that the highest stress concentrations occurred at the points where our scissors were connected to the springs. This observation highlighted potential weak points or structural vulnerabilities. Additionally, we noted a rapid increase in von Mises stress, indicating that the material was undergoing significant strain. Importantly, we found that the yielding strength of the material exceeded our expectations, suggesting robustness that could be exploited for optimization purposes.

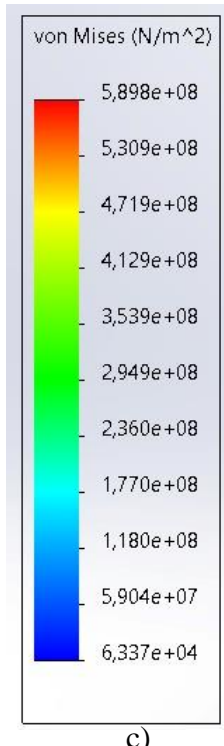
To achieve the desired angles, we used the displacement values obtained from the formulas within our kinematic model. This process allowed us to determine the necessary adjustments required to achieve the specified angles accurately. Furthermore, by analyzing the relationship between displacement and applied force, we gained valuable insights into the mechanical behavior of the system. This understanding enabled us to make informed decisions regarding force application and structural stability, thereby contributing to the overall efficacy of our analysis and design process.



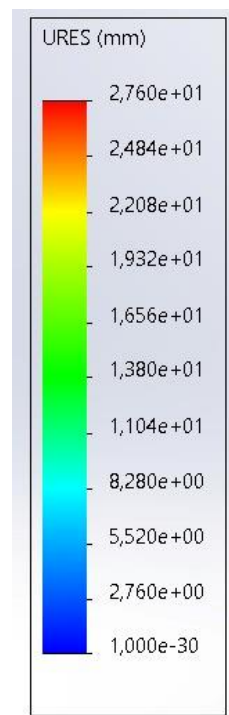
a)



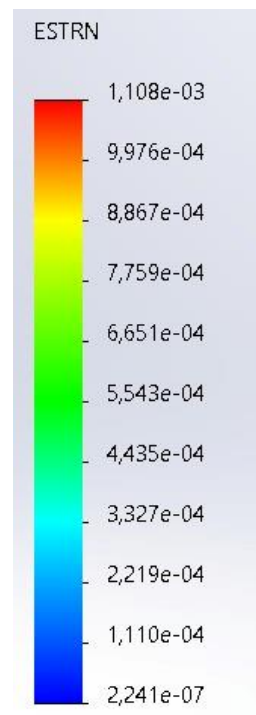
b)



c)



d)



e)

Figure 18: a and b) Analysis for 15 degrees c) Von mises values for 15 degrees d) Distance values for 15 degrees e) estrn values for 15 degrees

11.7. Optimization

Since the design phase was carried out alongside production, our design was shaped according to the manufacturing process. However, our research revealed that better results could be achieved with improved materials and certain refinements. According to these findings, we concluded that we could create a superior design.

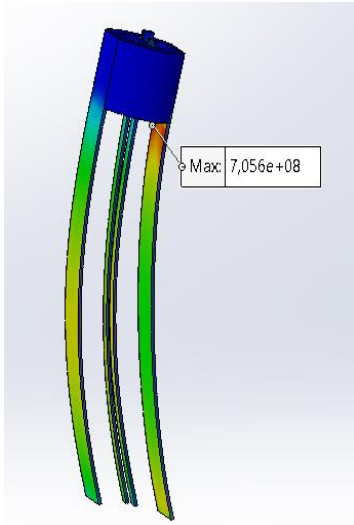
Our analyses showed that by changing the material, we could increase the rotation angle of our product. This is because the material we analyzed has greater flexibility. However, we couldn't proceed with production using this material, as sourcing nickel-titanium was challenging both in terms of cost and availability.

Our work has demonstrated that we can achieve the desired angle. The maximum achievable angle increased when compared to the stainless spring steel we initially used, and as a result, nickel-titanium would be a more suitable material. The results of our analysis using nickel-titanium are shown in the figure.

With the increased rotation angle, the design would be more convenient and practical for use in surgeries. Consequently, our design could be employed in more complex surgical procedures.

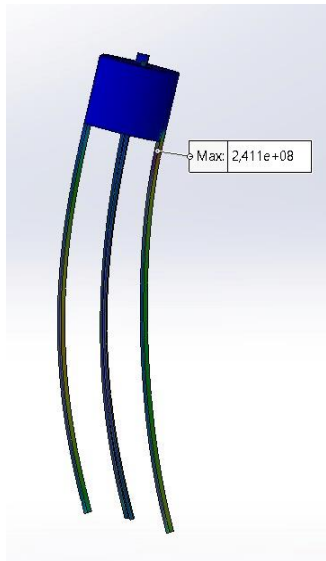
As seen in the figure, if we change the material to nickel titanium, the von mises values change. According to these results, if we use the material as nickel titanium, the maximum angle value we can reach will increase. The distortion angle will increase compared to stainless spring steel.

11.7.1. Comparison of nickel titanium and stainless spring steel



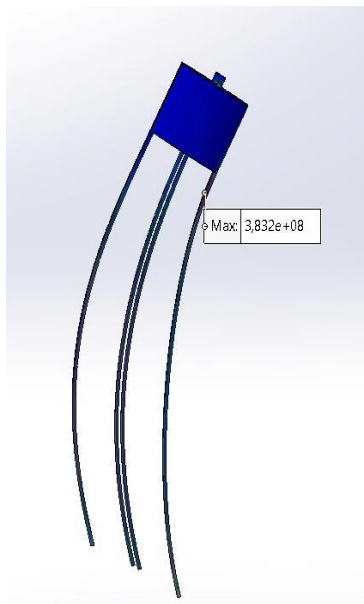
When we use stainless spring steel as the material at 30 degrees, it is seen that the maximum von mises value we achieve exceeds the yield strength by a very small amount. Therefore, when stainless spring steel is used, the maximum angle we can reach is approximately 30 degrees.

Figure 19: Max von mises values of stainless spring steel for 30 degrees



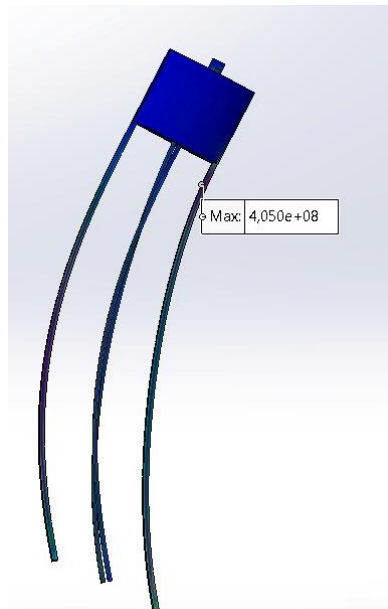
When we use nickel titanium as the material at 30 degrees, the maximum von mises value we obtain is below the yield strength of nickel titanium ($4 \times 10^8 \text{ N/m}^2$). With this result, it is more appropriate to use nickel titanium to optimize our robotic arm for a greater bending angle. When we bend both materials at 30 degrees, there will be a slight deformation in our stainless spring steel material, while there will be no deformation in our nickel titanium material.

Figure 20: Maximum Von mises values of nickel titanium for 30 degrees



When we use nickel titanium as the material at 45 degrees, the maximum von mises value we obtain is below the yield strength value of nickel titanium ($4 \times 10^8 \text{ N/m}^2$). With this result, it would be more appropriate to use nickel titanium to optimize our robotic arm for a greater bending angle. When we bend both materials at 45 degrees, there will be a lot of deformation in our stainless spring steel material, while there will be no deformation in our nickel titanium material.

Figure 21: Max Von mises values of nickel titanium for 45 degrees



When we use nickel titanium as the material at 57 degrees, the maximum von mises value we obtain is very close to the yield strength value of nickel titanium ($4 \times 10^8 \text{ N/m}^2$). As seen in the analysis, the maximum angle we obtain when spring stainless steel is used is approximately 30 degrees. It has been observed that when nickel titanium is used, this angle increases to approximately 57 degrees. Therefore, using nickel titanium in the production process will make the durability and elasticity of the material more useful.

Figure 22: Max Von mises values of nickel titanium for 57 degrees

11.7.2. Optimization of stainless spring steel according to its thickness

It is seen that the maximum angle value we obtain when we use stainless spring steel in the construction of the robotic arm is 30 degrees. In order to increase this angle, we obtained analyzes by changing the thickness of our springs as a different way than changing the material of the spring we use.

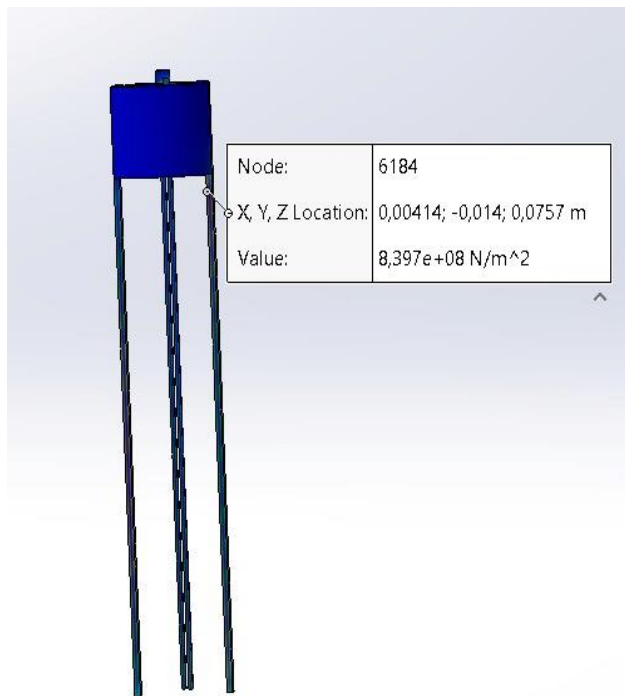


Figure 23: Analysis of stainless spring steel
with 2 mm thickness at 30 degree

First, we analyzed the thickness of our material as 2 mm, which is twice the normal thickness (1 mm). The results show that the maximum stress increases compared to the 1 mm material. The reason for this is that as the thickness of the material increases, it loses its elasticity and more force must be applied to reach the desired angle.

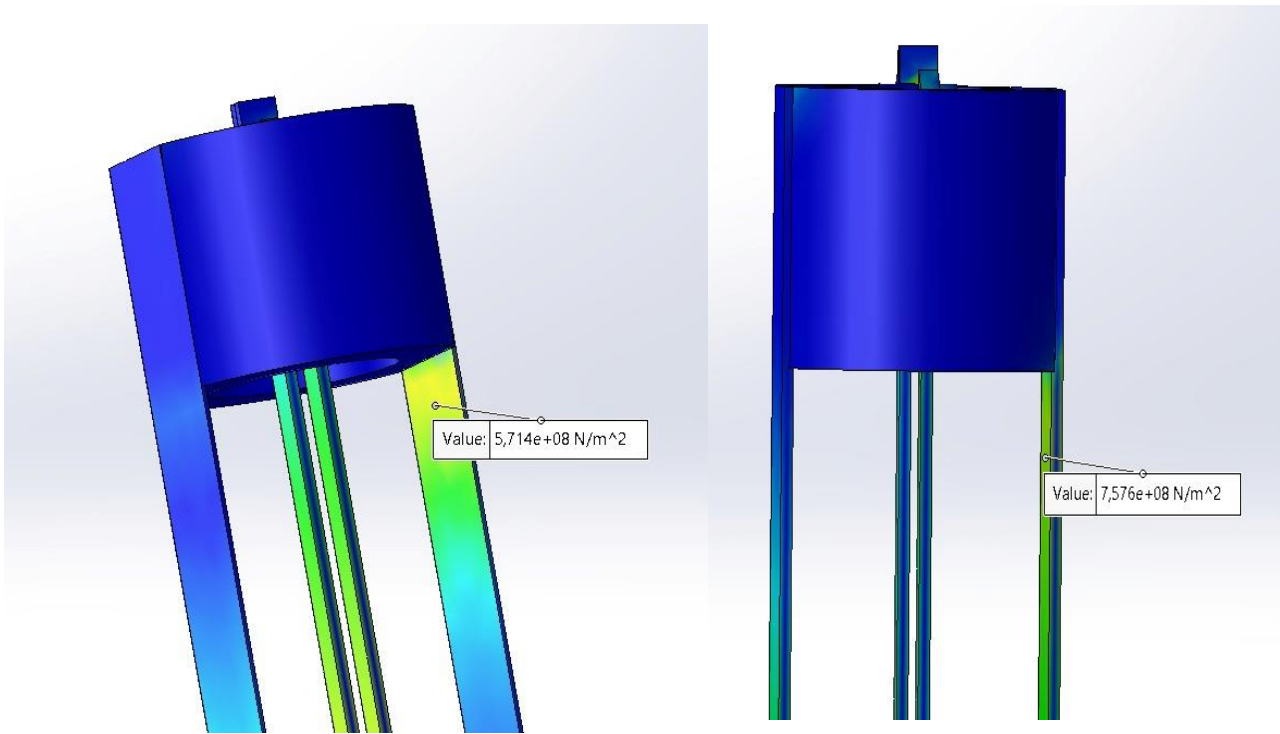


Figure 25: Analysis of stainless spring steel with 0,6 mm thickness at 30 degree

Figure 25: Analysis of stainless spring steel with 0,50 mm thickness at 30 degree

We analyzed how the thickness of our material would change when we first increased it and then decreased it. First, we reduced our thickness to 0.6 mm at 30 degrees. As a result of our analysis, when we reduced the thickness of our material, the stress level we observed remained below the yielding stress level, but when we reduced the thickness of our material to 0.5 mm. It has been observed that there is an increase compared to 0.6 mm. Based on these data, the thickness of our material should be more than 0.6 mm and less than 1 mm. Our material should not lose its elasticity and not be deformed.

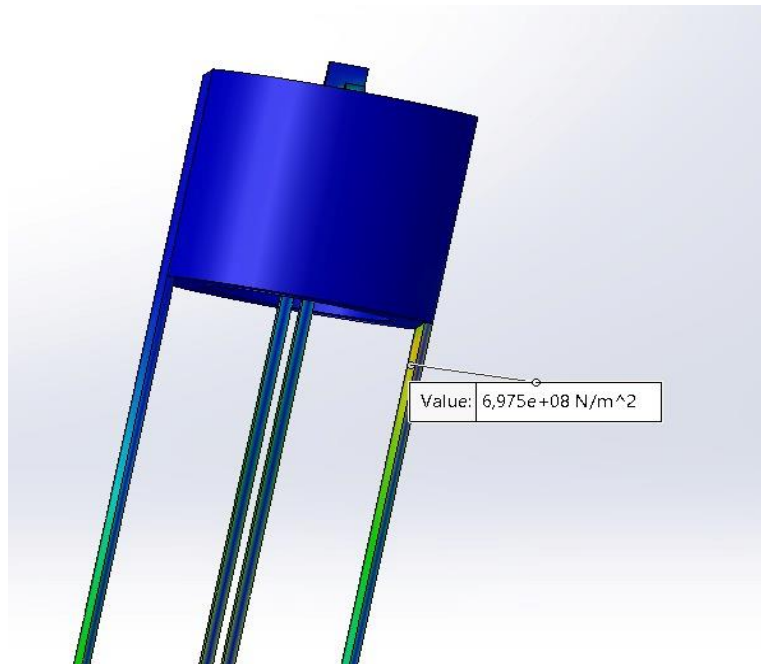


Figure 26: Analysis of the maximum angle that can be reached at 0.85 at 30 degrees

When the thickness of our material was analyzed between 0.6 mm and 1 mm, it was concluded that the best optimized thickness of our material was between 0.8 mm and 0.9 mm. In the analysis made with 0.85 mm in this range, it was observed that the maximum angle it could reach increased to approximately 42 degrees..

As a result of these analyses, we can increase the desired angle by changing the thickness of our material. In this scenario, the angle is increased by optimizing the thickness.

12. Work Space

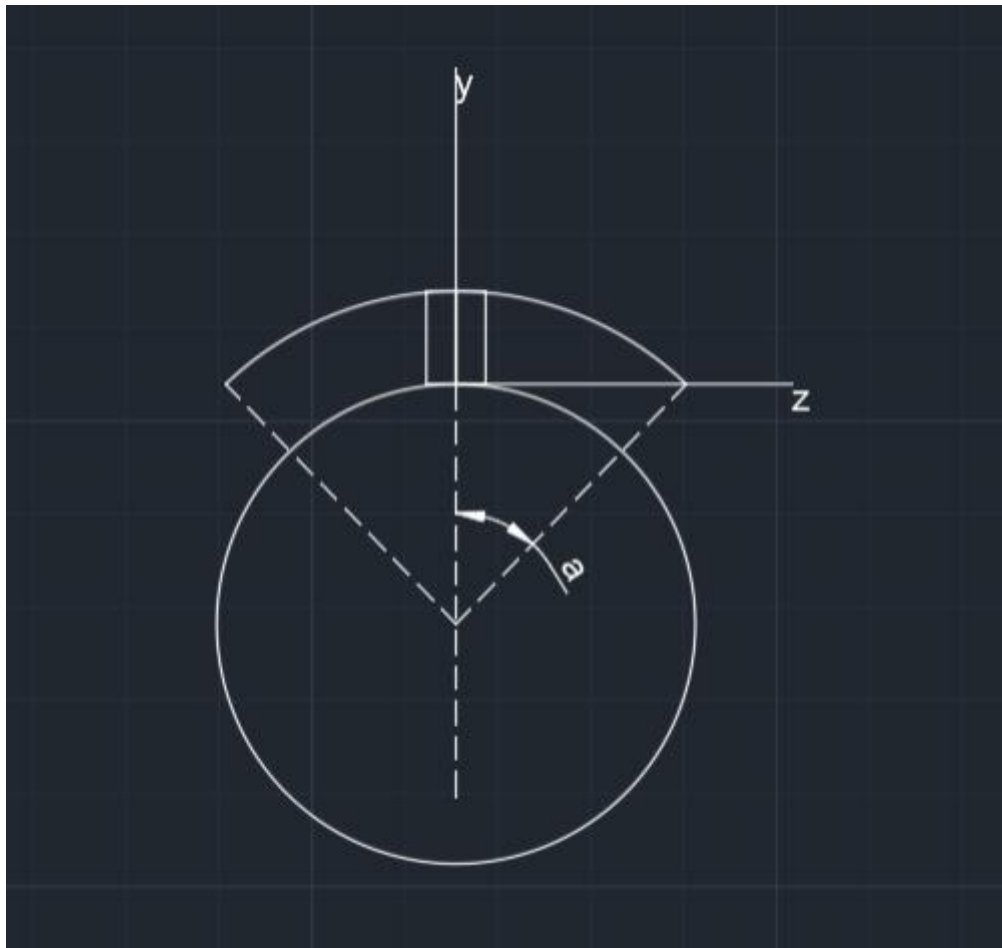


Figure 27: Scissor movement kinematic analysis

To compute our workspace, we relied on the kinematic models we crafted. Considering both the alpha and α angles, we meticulously determined the potential reach of our robotic surgical arm across the x, y, and z axes. Notably, we took into account distinct angles for both the scissors and the large springs, recognizing their unique contributions to the arm's maneuverability.

For each angle, we conducted thorough analyses to ascertain the displacements required to navigate our robotic surgical arm to specified positions within the x, y, and z coordinates. These calculations were meticulously tabulated, providing a comprehensive overview of the displacement requirements for achieving precise positioning in various scenarios.

By meticulously documenting these displacement values, we established a robust framework for guiding the arm to desired locations during operation. This meticulous approach ensures that the arm can effectively reach intended points within the workspace, facilitating precise and controlled movements crucial for successful surgical procedures.

At this point, we have calculated the movement of the scissors in the z axis by opening and closing with these formulas.

$$z = r \times \sin \alpha$$

As a result of the calculations made, we have the opportunity to see how much the scissors move in the z axis. At the same time, the movement of the scissors is not hindered while rotating. In Table 2, you see how much the scissors moves in the z axis according to the angle.

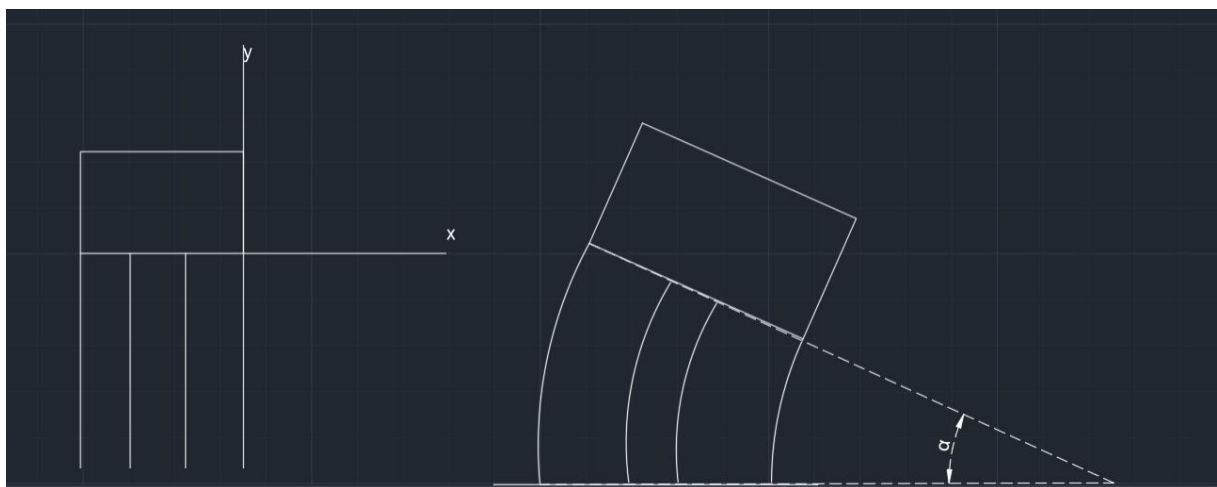


Figure 28:work space drawing with AutoCAD

$$\text{arc length} = (200 - 30) - L_{a1} \quad (21)$$

$$r = \frac{\text{arc length} * 360}{2\pi a} \quad (22)$$

$$\text{movement on y axis} = (200 - 30) * \sin(a) * r \quad (23)$$

$$\text{movement on x axis} = r - (r * \cos(a)) \quad (24)$$

r: radius of the center of bend

a: alpha angle (bending angle)

arc length: length of bent spring(200 mm is L and 30 mm is distance of endpoint from x-axis)

For 30 degree example:

$$a = 30 \text{ degree}$$

$$L_{a1} = 8,66 \text{ taking table 1}$$

$$\text{arc length} = (200 - 30) - 8,66 = 161,34 \text{ mm}$$

$$r = \frac{\text{arc length} * 360}{2\pi a} = 308,14 \text{ mm}$$

$$\text{movement on y axis} = (200 - 30) * \sin(a) * r = 170 * \sin 30 * 308,14 = 15,93 \text{ mm}$$

$$\text{movement on x axis} = r - (r * \cos(a)) = 308,14 - (308,14 * \cos(30)) = 41,28 \text{ mm}$$

$$\sqrt{15,93^2 + 41,28^2} = \sqrt{1957,8} = 44,25 \text{ mm}$$

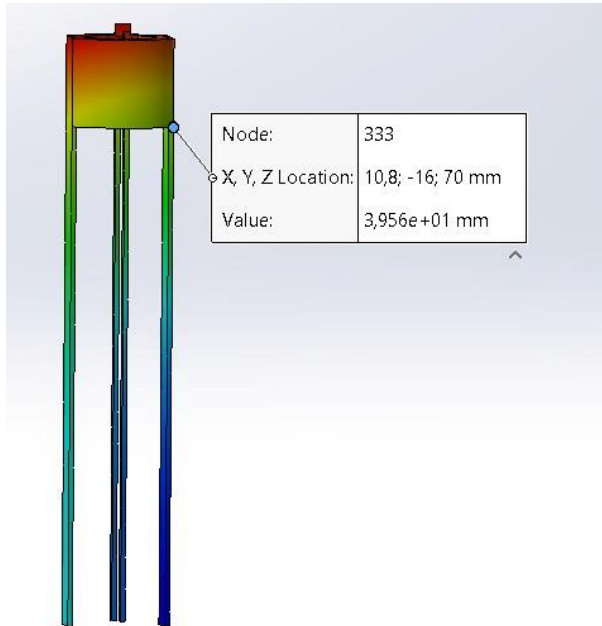


Figure 29:analysis of 30 degree displacement

These results were calculated according to 30 degrees. When compared in the analysis section, it was seen that there was an error margin of approximately 11 percent. The reason for this error was factors such as the quality and number of mesh used in the analysis. The result of the analysis for 30 degrees is given in the figure below.

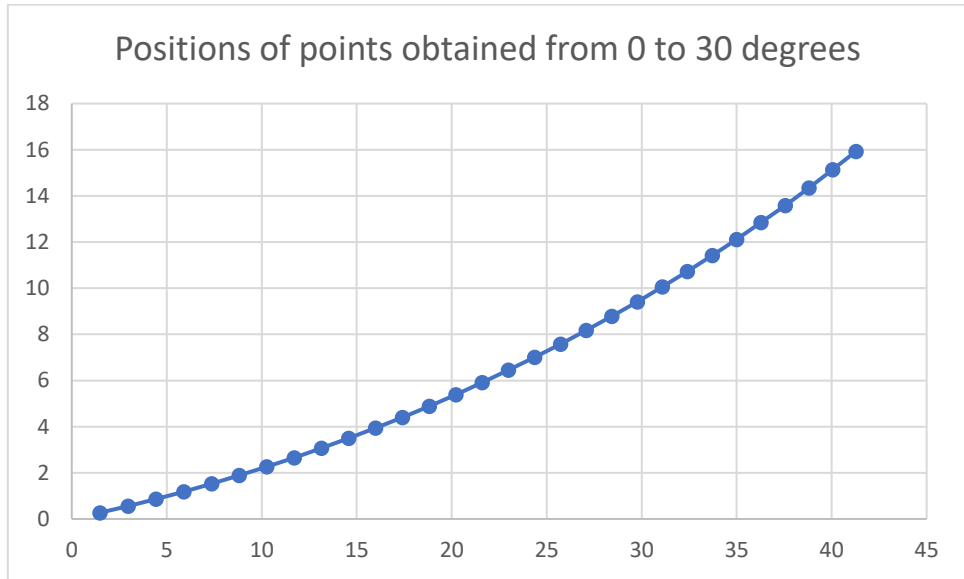
$$\text{error calculation} = \frac{44,25 - 39,56}{39,56} * 100 = \%11,1$$

The calculations based on alpha values are given in the table below. An example of these calculations is shown above. The values in the table are calculated with the help of Excel and presented to the user.

Table 2:Table of work space according to alpha degree

a(degree)	Arc Length (mm)	radius(mm)	Movement on y axis(mm)	Movement on x axis(mm)	Movement on z axis(mm)
1	169,74	9725,28	0,27	1,48	0,09
2	169,48	4855,14	0,56	2,96	0,17
3	169,21	3231,75	0,86	4,43	0,26
4	168,95	2420,05	1,19	5,90	0,35
5	168,69	1933,02	1,53	7,36	0,44
6	168,42	1608,33	1,88	8,81	0,52
7	168,16	1376,39	2,26	10,26	0,61
8	167,89	1202,44	2,65	11,70	0,70
9	167,62	1067,13	3,06	13,14	0,78
10	167,36	958,87	3,49	14,57	0,87
11	167,08	870,29	3,94	15,99	0,95
12	166,81	796,47	4,41	17,40	1,04
13	166,54	733,99	4,89	18,81	1,12
14	166,26	680,43	5,39	20,21	1,21
15	165,98	634,00	5,91	21,60	1,29
16	165,70	593,37	6,45	22,99	1,38
17	165,41	557,50	7,00	24,36	1,46
18	165,13	525,61	7,58	25,73	1,55
19	164,84	497,07	8,17	27,08	1,63
20	164,54	471,37	8,78	28,43	1,71
21	164,24	448,11	9,41	29,76	1,79
22	163,94	426,96	10,06	31,09	1,87
23	163,63	407,63	10,73	32,40	1,95
24	163,32	389,90	11,41	33,71	2,03
25	163,01	373,58	12,12	35,00	2,11
26	162,68	358,50	12,84	36,28	2,19
27	162,36	344,53	13,59	37,55	2,27
28	162,02	331,55	14,35	38,81	2,35
29	161,69	319,44	15,13	40,05	2,42
30	161,34	308,14	15,93	41,28	2,50

Table 3: Positions of points obtained from 0 to 30 degrees



13. Manufacturability

First of all, because we wanted a sprain, a suitable material search was conducted for it. We tried some of the materials we found and we couldn't find the materials we wanted. The materials we found did not deform immediately and return to their former state. At the end of our research, a material was found in IMES in the way we wanted in the Yaybant company. This material was stainless spring steel and provided exactly the movement we wanted. After taking a few samples, we came to the conclusion as a result of the analysis which sample is the best suitable for our design and which is the right one. To supply stainless spring steel with a thickness that matches our analysis. And thickness 1.5mm we have cut stainless spring steel so that its length is 400 mm and its width is 20 mm.



Figure 30: first cylinder (head part)

Then we walked around the industrial street to produce the cylinder, which will be found in the most extreme part. We had the opportunity to produce this part in a company. This cylinder, which was made of chrome-plated spindle material, felt much heavier than it should have been. We made an analysis of this product with our design, but it was decided to give up this material and design it with different materials because it would be really heavy. We have come to the conclusion that it will be possible to install stainless spring steels to the thickness of this cylinder only by using wire erosion. As a result of the negotiations we have made, the wire erosion is quite costly and the thickness is low we have received his return, which he will have to deal with a lot because it cannot be done. Therefore, by changing the design, we have opened a slot so that stainless spring steel can enter the surface of the cylinder.

After this design change, we have ensured the production of the cylinder at the tip by using a 3D printer for the purpose of experimenting. As a result of the experiments we conducted, it was seen that the design we made was correct.

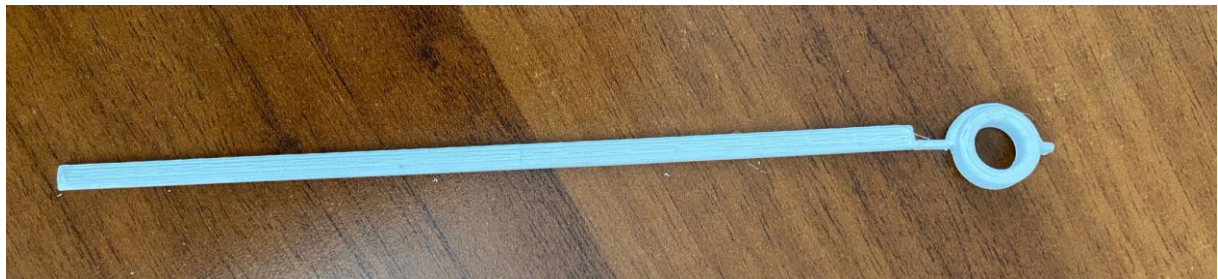


Figure 31: 3D printer prototype of scissors

In order to be more robust and convenient, the cylinder at the tip was produced as an aluminum material on a CNC machine. Stainless spring steel screw holes were opened in accordance with the installation we tried to open these screw holes ourselves, but we could not do it because of the possibilities we had, we could not succeed because it is a very flexible material and at the same time there is no suitable drilling tip. Therefore, by requesting the cylinder from the place where we produced, the screw holes were opened and made ready for installation.



Figure 32: shaft and stainless steels mounted on the cylinder

The shaft, which is the future of scissors, was also produced where we produced the cylinder.

We have provided the production of scissors primarily for trial purposes again with the help of a 3d printer. As a result of the experiments we conducted, it was seen that it was suitable for our design by providing the movement of the scissors. After we realized that it was suitable, we also made the production of scissors.

After all the parts were produced, it was time to assemble. We started the installation by first placing the shaft in the cylinder. Later, the necessary adjustments were made so that the scissors would rotate on the shaft. Then we mounted the stainless spring steels with the screw holes open to the cylinder with the help of the M5 screw. After installation, we also had the opportunity to try out the second cylinder that we mentioned in the design section. We also had successful results in our experiments with the second cylinder. It was quite gratifying that it could also be used in this way.

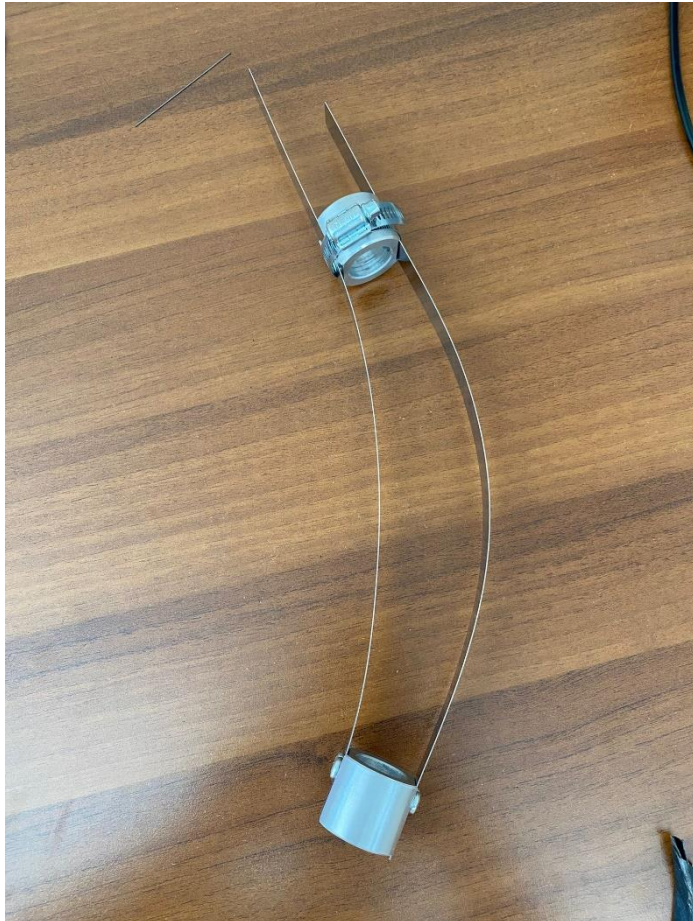


Figure 34: production of design



Figure 34: Assembly of the second cylinder design

14. Discussion and Conclusion

The aim of this project is to make the robotic surgical arm, which is very costly and difficult to produce, less costly and easier to produce. Our other aim is to enable the robotic arm to make the desired movements and be easily brought to the desired position. Our design and production meet these criteria in the best way.

We carried out our analysis and production for this purpose in this project. We encountered many difficulties in this process. The first of these difficulties is the production part. Since our resources in the production part were limited, we had to change the designs we made several times. We asked for help from industries and factories in this process. We were able to obtain the materials we used in the design. We went to many different workshops for the analysis part. In the analysis part, we received support from many people and institutions who are professionals in this field and work in this sector. We created our analyzes and formulas in this direction. When the results we found with the formulas were compared with the results we found in the analysis part, we obtained close results. The error margins we used in the analysis part This is due to the inadequacy of the facilities we have in providing and running the programs. When better computers and higher quality mesh and number are used, the margin of error will decrease.

As a result of our analysis, the reactions of the robotic arm in different positions and angles were reached. As a result, the limits of our material were determined. Different materials can be used to increase the limits and durability of the robotic arm. For example, Ni-Ti is used in many different robotic surgery arm projects, but due to high cost and accessibility problems, this material is used. We could not use it. The material we use is very successful in terms of flexibility and durability. It is better than other materials in terms of cost and accessibility.

We carried out our design and production in parallel. In this context, we had to make some changes in the design part due to the problems we encountered during the production phase. When better production conditions and material supply are provided, the design part can be designed more successfully and on demand.

As a result, we took an active part in the design, production and analysis parts of a device in this project. We encountered many difficulties at these stages. We approached these problems with rational solution suggestions. We gained a lot of knowledge and experience during these processes.

15. References

- 3.5 mm compliant robotic surgical forceps with 4 DOF : design and performance evaluation D. S. V. Bandara, Ryu Nakadate, Murilo M. Marinho, Kanako Harada, Mamoru Mitsuishi & Jumpei Arata
- Sensored Surgical Forceps for Robotically Assisted Minimally Invasive Surgery Authors: Kim, Uikyum; Kim, Yong Bum; So, Jinho; Seok, Dong-Yeop; Choi, Hyouk Ryeol
- Lyapunov-based bilateral teleoperation for surgical robotic forceps system with time varying delay Authors: Ishii, Chiharu; Mikami, Hiroyuki; Nishitani, Yosuke
- A New Type of Surgical Forceps Integrated with Three-Axial Force Sensor for Minimally Invasive Robotic Surgery Authors: Kim, Uikyum; Kim, Yong Bum; Seok, Dong-Yeop; So, Jinho; Choi, Hyouk Ryeol
- Force Sensor Integrated Surgical Forceps for Minimally Invasive Robotic Surgery Authors : Kim, Uikyum; Lee, Dong-Hyuk; Yoon, Woon Jong; Hannaford, Blake; Choi, Hyouk Ryeol
- Meta-analysis of observational studies on the safety and effectiveness of robotic gynaecological surgery Authors:M. Reza; S. Maeso; J. A. Blasco; E. AndradasM. Reza; S. Maeso; J. A. Blasco; E. Andradas
- Transanal specimen extraction in robotic rectal cancer surgery Authors:J. Kang; B. S. Min; H. Hur; N. K. Kim; K. Y. Lee
- <https://www.ncbi.nlm.nih.gov/pmc/articles/PMC6261744/#:~:text=The%20idea%20of%20robotics%20used,use%20in%20prosthetic%20hip%20replacement>.
- An Articulated Robotic Forceps Design With a Parallel Wrist-Gripper Mechanism and Parasitic Motion Compensation
- Multifunctional Robotic Surgical Forceps With Tactile Sensor Array for Enhanced Palpation and Clamping
- Compact 4DOF Robotic Forceps With 3.5 mm Diameter for Neurosurgery
- Force Feedback Control of Robotic Forceps for Minimally Invasive Surgery
- Portable manipulation system for commercial robotic surgery forceps
- Kirchhof B, Wong D. Vitreo-retinal surgery. Springer; 2005

- Tano Y, Kamei M, Ooji M, Saitou Y, Won PI, Lewis JM. Membrane eraser. Jul, 1999.
- Ueta, Yamaguchi Y, Shirakawa Y, Nakano T, Ideta R, Noda Y, Morita A, Mochizuki R, Sugita N, Mitsuishi M. Robot-assisted vitreoretinal surgery development of a prototype and feasibility studies in an animal model. *Ophthalmology*. 2009 Aug;116:1538–1543.e2.
- Riviere C, Ang WT, Khosla P. Toward active tremor canceling in handheld microsurgical instruments. *Robotics and Automation, IEEE Transactions on*. 2003 Oct;19:793–800.
- Uneri A, Balicki M, Handa J, Gehlbach P, Taylor R, Iordachita I. New steady-hand eye robot with micro-force sensing for vitreoretinal surgery. *Biomedical Robotics and Biomechatronics (BioRob), 2010 3rd IEEE RAS and EMBS International Conference on*; sept. 2010. pp. 814–819
- Karacorlu M, Karacorlu S, Ozdemir H. Iatrogenic punctate chorioretinopathy after internal limiting membrane peeling. *American Journal of Ophthalmology*.
- Gupta P, Jensen P, de Juan E. Surgical forces and tactile perception during retinal microsurgery. In: Taylor C, Colchester A, editors. *Medical Image Computing and Computer-Assisted Intervention (MICCAI'99)* vol 1679 of *Lecture Notes in Computer Science*. Springer; Berlin / Heidelberg: 1999. pp. 1218–1225.
- Berkelman P, Whitcomb L, Taylor R, Jensen P. A miniature microsurgical instrument tip force sensor for enhanced force feedback during robot-assisted manipulation. *Robotics and Automation, IEEE Transactions on*. 2003 Oct;19:917–921.
- Jagtap A, Riviere C. Applied force during vitreoretinal microsurgery with handheld instruments. *Engineering in Medicine and Biology Society, 2004 IEMBS '04 26th Annual International Conference of the IEEE*. 2004 Sep;1:2771–2773.
- Sun Z, Balicki M, Kang J, Handa J, Taylor R, Iordachita I. Development and preliminary data of novel integrated optical micro-force sensing tools for retinal microsurgery. *Robotics and Automation. ICRA '09. IEEE Int. Conf. on*; 2009. pp. 1897–1902
- Iordachita I, Sun Z, Balicki M, Kang J, Phee S, Handa J, Gehlbach P, Taylor R. A sub-millimetric, 0.25 mn resolution fully integrated fiber-optic force-sensing tool for retinal microsurgery. *International Journal of Computer Assisted Radiology and Surgery*. 2009;4:383–390.

- https://en.wikipedia.org/wiki/Robot-assisted_surgery
- https://en.wikipedia.org/wiki/Da_Vinci_Surgical_System